UPPSALA
UNIVERSITET

Digital Comprehensive Summaries of Uppsala Dissertations from the Faculty of Science and Technology 1499

Resource characterization and variability studies for marine current power

NICOLE CARPMAN

ACTA
UNIVERSITATIS
UPSALIENSIS
UPPSALA
2017

ISSN 1651-6214
ISBN 978-91-554-9881-8
urn:nbn:se:uu:diva-319033

Dissertation presented at Uppsala University to be publicly examined in Häggsalen, Ångströmlaboratoriet, Uppsala, Wednesday, 31 May 2017 at 09:15 for the degree of Doctor of Philosophy. The examination will be conducted in English. Faculty examiner: Professor AbuBakr S. Bahaj (University of Southampton, Engineering and the Environment).

Abstract

Carpman, N. 2017. Resource characterization and variability studies for marine current power. *Digital Comprehensive Summaries of Uppsala Dissertations from the Faculty of Science and Technology* 1499. 64 pp. Uppsala: Acta Universitatis Upsaliensis. ISBN 978-91-554-9881-8.

Producing electricity from marine renewable resources is a research area that develops continuously. The field of tidal energy is on the edge to progress from the prototype stage to the commercial stage. However, tidal resource characterization, and the effect of tidal turbines on the flow, is still an ongoing research area in which this thesis aims to contribute.

In this thesis, measurements of flow velocities have been performed at three kinds of sites. Firstly, a tidal site has been investigated for its resource potential in a fjord in Norway. Measurements have been performed with an acoustic Doppler current profiler to map the spatial and temporal characteristics of the flow. Results show that currents are in the order of 2 m/s in the center of the channel. Furthermore, the flow is highly bi-directional between ebb and flood flows. The site thus has potential for in-stream energy conversion. Secondly, a river site serves as an experimental site for a marine current energy converter that has been designed at Uppsala University and deployed in Dalälven, Söderfors. The flow rate at the site is regulated by an upstream hydro power plant, making the site suitable for experiments on the performance of the vertical axis turbine in a natural environment. The turbine was run in steady discharge flows and measurements were performed to characterize the extent of the wake. Lastly, at an ocean current site, the effect that transiting ferries may have on submerged devices was investigated. Measurements were conducted with two sonar systems to obtain an underwater view of the wake caused by a propeller and a water jet thruster respectively.

Furthermore, the variability of the intermittent renewable sources wind, solar, wave and tidal energy was investigated for the Nordic countries. All of the sources have distinctly different variability features, which is advantageous when combining power generated from them and introducing it on the electricity grid. Tidal variability is mainly due to four aspects: the tidal regime, the tidal cycle, local bathymetry causing turbulence, asymmetries etc. and weather effects. Models of power output from the four sources was set up and combined in different energy mixes for a “highly renewable” and a “fully renewable” scenario. By separating the resulting power time series into different frequency bands (long-, mid-, mid/short-, and short-term components) it was possible to minimize the variability on different time scales. It was concluded that a wise combination of intermittent renewable sources may lower the variability on short and long time scales, but increase the variability on mid and mid/short time scales.

The tidal power variability in Norway was then investigated separately. The predictability of tidal currents has great advantages when planning electricity availability from tidal farms. However, the continuously varying tide from maximum power output to minimum output several times per day increases the demand for backup power or storage. The phase shift between tidal sites introduces a smoothing effect on hourly basis but the tidal cycle, with spring and neap tide simultaneously in large areas, will inevitably affect the power availability.

Keywords: Marine current energy, tidal currents, wake, variability, renewable energy, ADCP, flow measurement

Nicole Carpman, Department of Engineering Sciences, Electricity, Box 534, Uppsala University, SE-75121 Uppsala, Sweden.

ISSN 1651-6214
ISBN 978-91-554-9881-8
urn:nbn:se:uu:diva-319033 (http://urn.kb.se/resolve?urn=urn:nbn:se:uu:diva-319033)

For those who see with their own
eyes and feel with their own hearts

Inspired by Albert Einstein

List of Papers

This thesis is based on the following papers, which are referred to in the text by their Roman numerals.

I **Carpman, N.** and Leijon, M. (2014) "Measurements of tidal current velocities in the Folda Fjord, Norway, with the use of a vessel mounted ADCP". *Proceedings of the ASME 2014 33rd International Conference on Ocean, Offshore and Arctic Engineering, Volume 8A: Offshore Engineering,* San Francisco, California, USA, June 8-13, 2014.

II **Carpman, N.** and Thomas, K. (2016) "Tidal resource characterization in the Folda Fjord, Norway". *International Journal of Marine Energy,* 13 pp 27-44.

III Lundin, S., Forslund, J., **Carpman, N.**, Grabbe, M., Yuen, K., Apelfröjd, S., Goude, A. and Leijon, M. (2013) "The Söderfors project: Experimental hydrokinetic power station deployment and first results". *Proceedings of the 10th European Wave and Tidal Energy Conference,* Aalborg, Denmark, September 2-5, 2013.

IV Lundin, S., **Carpman, N.**, Thomas, K. and Leijon, M. (2015) "Studying the wake of a marine current turbine using an acoustic Doppler current profiler". *Proceedings of the 11th European Wave and Tidal Energy Conference,* Nantes, France, September 6-11, 2015.

V Francisco, F., **Carpman, N.**, Dolguntseva, I. and Sundberg, J. "Observation of cavitating flow using multibeam and dual-beam sonar systems: A comparison of wake strength caused by propeller vs waterjet thrusted vessels. In a marine renewable energy perspective (Part-a)". *Resubmitted after revision to Journal of Marine Science and Engineering, April 2017.*

VI Widén, J., **Carpman, N.**, Castellucci, V., Lingfors, D., Olauson, J., Remouit, F., Bergkvist, M., Grabbe, M. and Waters, R. (2015) "Variability assessment and forecasting of renewables: A review for solar, wind, wave and tidal resources". *Renewable & Sustainable Energy Reviews*, 44 pp 356-375.

VII Olauson, J., Ayob, M.N., Bergkvist, M., **Carpman, N.**, Castelluci, V., Goude, A., Lingfors, D., Waters, R. and Widén, J. (2016) "Net load variability in Nordic countries with a highly or fully renewable power system". *Nature Energy* Vol. 1 pp 1-8.

VIII **Carpman, N.** and Thomas, K. (2016) "Tidal current phasing along the coast of Norway". *Proceedings of the 3rd Asian Wave and Tidal Energy Conference*, Singapore, October 24-28, 2016.

Reprints were made with permission from the respective publishers.

Table of Contents

Nomenclature

Notation	Description	Unit
A	Area	m^2
D	Turbine diameter	m
H	Tidal range	m
H_i	Tidal amplitude for tidal constituent *i*	m
N	Number of pings per ensemble	
T	Period time	s
U	Velocity	m/s
U_{max}	Peak speed at turbine hub height	m/s
P	Power	W
h	Measured depth	m
h_0	Reference water level	m
p	Air pressure	hPa
t_{lag}	Time lag	s
u	North-component of velocity	m/s
v	East-component of velocity	m/s
v_{norm}	Undisturbed flow speed	m/s
v_{def}	Speed deficit	m/s
w	Vertical component of velocity	m/s
z	Water surface elevation	m
ρ	Water density	kg/m^3
σ	Standard deviation	
φ	Tidal phase	

Abbreviations	
ADCP	Acoustic Doppler Current Profiler
DBS	Dual Beam System
GNSS	Global Navigation Satellite System
GPS	Global Positioning System
IRE	Intermittent Renewable Energy
LT	Long-term
MBS	Multi Beam System
MST	Mid/Short-term
MT	Mid-term
PG	Percent Good
RTK	Real Time Kinematic
ST	Short-term

1. Introduction

The interest in, and economic market for, converting energy from renewable resources into electricity is continuously growing around the world. In recent years, the development of marine current energy conversion systems has intensified. Most suitable for deploying in-stream tidal turbines are sites with high tidal current velocities. However, for the tidal-stream energy industry to be fully realized, lower velocity sites should also be utilized.

Tides have the advantage of being predictable decades ahead. However, the tidal resource is intermittent and has local variations that affect the power output from a conversion system. Each potential site is unique; the velocity flow field at a tidal site is highly influenced by local bathymetry and turbulence. Hence, characterizing the resource requires careful investigations and providing high quality velocity data from measurement surveys is of great importance for developers and researchers in the field of tidal current energy.

This thesis covers two main aspect of marine current energy. Firstly, measurements and characterizations of tidal currents, turbine wakes and ship wakes. Secondly, investigation of the variability in power output from the intermittent renewable energy sources wind, solar, wave and, in particular, tidal energy, including an investigation of how these can be combined to reduce the variability in the power production to the grid in a future energy mix.

1.1 Research objectives

The main objective of this thesis was to contribute to the development of measurement techniques and characterizing methods of flow velocity data, with the aim to increase the overall understanding of marine currents as a renewable energy resource. Furthermore, the research aimed to provide a broader understanding of effects concerning energy conversion with in-stream turbines, through investigation of the wake effect of a demonstration prototype. Also the possible effect on submerged turbines due to transiting ships in shallow straits was investigated.

Looking into the future, the probable course of development is towards an energy system with an increasing share of electricity from renewable and intermittent energy sources like wind, solar, wave and tidal power. In the light of this matter, this work investigated how variable renewable sources can be combined in a future energy mix without introducing a high variability in the

electricity system, especially in what respect the phase shift of tides can be utilized when aggregating different tidal farms to minimize the variability and also how it may be used to smooth out variations of other intermittent energy sources.

1.2 Layout of thesis

This doctoral thesis first describes the work performed on characterizing marine currents in three types of sites; a river site, a tidal site and an ocean current site. The main contribution of the author has been to perform measurement surveys of flow velocities at these various locations and, through analysis of measurement data, describe flow characteristics and/or resource potential.

Papers I and II cover a tidal site in Norway that has been investigated as a potential tidal energy site. Papers III and IV cover a river site which is part of the Söderfors project where a first survey to characterize the wake has been performed. In Paper V, cavitation-induced turbulence in the wake of transiting ferries is investigated. In Papers VI, VII and VIII, the variability of renewable resources are studied. First, the variability of the natural resources (wind, solar, wave and tidal) is reviewed, then the combination of power output from these sources, and how they would affect the variability on the electrical grid in the Nordic countries, was studied. At last, an investigation is presented on how an aggregation of tidal sites with different tidal phase in Norway could be used to smooth out the variability in power output over a large area.

The layout is as follows. Chapter 2 provides the reader with background to marine current power, the characteristics of tides, cavitation and variability. In Chapter 3, the instruments used for current and turbulence measurements are presented. In Chapter 4, general aspects of the methodology for resource potential assessment are described followed by a description of site specific methodology from field work. Then research performed on variability from all of the renewable sources and tidal variability specifically is presented. The results are presented in Chapter 5 for each research area with conclusions stated in Chapter 6.

2. Background and theory

2.1 Marine current power

Conventional hydro power plants have long been used to generate electricity. Lately, the interest in and aim for using other forms of water motions as a source of renewable energy has intensified. Many countries are aiming for a more sustainable energy production [1] where marine current power from tidal energy is one of the important areas of research. Other sources of marine currents are unregulated rivers and ocean currents where the same technology could be used.

The technical development of in-stream converters of tidal currents is continuously progressing. The leading technical solution is horizontal axis turbines with two, three[1] or more[2] blades, submerged in the water either at bottom foundations or placed on towers [2]. However, tidal energy is still in an early stage of development. The majority of produced energy comes from a few large tidal barrage projects [3]. In-stream technology is still in the prototype and demonstration stage and has not yet developed into a commercial market. Nevertheless, a number of new projects are ongoing, mainly in Europe and East Asia [4].

The understanding of tidal hydrokinetic energy and the effect on the flow when extracting such energy with single turbines or larger farms have been developed by e.g. [5–14]. When a potential site has been localized, one of the first steps in a tidal energy project is resource assessment, either by numerical modeling or in-field measurements. Around the world, numerous investigations have been performed where the water velocity field has been measured and characterized, see e.g. [15–31]. Different aspects have been discussed such as directionality [32–35], tidal asymmetry [15,36] and non-tidal effects of tides and currents such as winds, waves and pressure [37–40].

The hydrokinetic power density per cross-sectional area (W/m^2) is given by

$$\frac{P}{A} = \frac{\rho U^3}{2} \qquad \text{(Eq. 1)}$$

The power available in streaming water is scaling up fast with velocity, U, due to the cubic relationship, but even at low velocities the power is substantial

[1] Nova Innovation Ltd. https://www.novainnovation.com/ <2017-02-20>
[2] Atlantis Resources. https://www.atlantisresourcesltd.com/ <2017-02-20>

due to the high density of water, ρ (1025 kg/m^3, corresponding to 800 times that of air). However, when energy conversion systems like turbines are introduced, one has to take into account the properties of each converter. For large farms, the number of devices and formation of rows are also of importance [14]. Moreover, extracting power from a flow will affect the flow itself [6,9,22,41,42].

One important aspect of any renewable energy resource is its variability. To get a firm electric power output, the resource should preferably be of equal magnitude all of the time and easy to forecast. Tides, for example, are easy to forecast but they are by nature fluctuating from peak speeds to near zero velocities several times per day (see Section 2.2), thus, resulting in a varying power output from a conversion system. When tidal turbines extract power from the flow, this changes not only the flow speed but also the phase of the tide [43]. When tidal current power is part of the energy mix together with other renewable energy sources like wind, solar and wave power, the variability in power output from all of these natural resources needs to be combined and accounted for and ultimately compensated for to maintain a firm electricity production. This matter is further discussed in Sections 2.5 and 4.3.

At Uppsala University the marine current group is working on the Söderfors project where a marine current energy converter prototype has been developed and deployed at a test site in a river. The site is located just downstream of a hydro power plant. Thus, it is a suitable site for performing experiments since the flow discharge in the channel is regulated by the hydro power plant and can be kept steady during experiments. The flow at the site was investigated by Lalander et al. in [44,45]. The converter is based on a robust technique, i.e. a vertical axis marine current turbine and a permanent magnet synchronous generator, intended to operate from a cut in speed of 0.6 m/s and depths from around 7 m as described in Paper III and [46,47]. The marine current energy converter has been tested for performance [48,49] and wake effects (Paper IV). Moreover, a load control system is being developed [50] and a grid integration system has been investigated [51]. Several doctoral theses have come out of this project [52–58]. Previous work has included analyses of the tidal current energy resource in Norway [53,59].

2.2 Tides and tidal currents

Tides are the periodic variations of sea level elevations. It is due to gravitational forcing from the Sun and the Moon in interaction with the rotation of the Earth. The tidal regime is most commonly semidiurnal with two highs and two lows each day, but can also be diurnal with one high and one low or a mix of the two [60]. As a renewable energy resource, tides have the advantage of being predictable decades ahead. The predicted astronomical tide, h, at a site

can be expressed as a sum of harmonic constituents representing variations of different amplitude and time scale, according to

$$h = h_0 + \sum_i H_i \cos\left(\frac{2\pi}{T_i} + \varphi_i\right) \quad \text{(Eq. 2)}$$

where h_0 is the reference water level relative to the mean sea level and each constituent i corresponds to a tidal amplitude H, period T and phase φ. Information and forecasts of tidal heights are publically available in tidal charts for most areas around the world.

The moon exerts the strongest forcing. The principal lunar semidiurnal constituent is called M_2 and has a period of 12 hours 25 minutes. The principal solar semidiurnal constituent S_2 has a period of 12 hours. These are in phase every fortnight (14.76 days) forming spring tides, with neap tides in between (when the misalignment is 90°) [61]. Multiples of these or shallow water constitutes further alter the symmetry and phase of the tidal cycle. To resolve all relevant constituents, at least 29 days of observations are needed.

The tidal waves propagate around the oceans, with a smooth variation over distances on the order of 100 km, and give rise to floods and ebbs in the coastal areas. The rising and falling sea levels produce tidal currents. Strong currents occur if a large amount of water is being pushed through a fjord inlet, a strait, a sound between two islands or around a headland. These currents are enhanced in areas where depth and width are restricted due to bathymetry. A higher tidal range gives faster current acceleration and higher maximum speed, and thus a higher variability.

Tidal currents at a site need to be measured to be correctly characterized since they are altered by effects such as drag from the bottom creating turbulence (i.e. chaotic flow filled with eddies of various sizes) and changing the flow path as well as the vertical profile. As shown in e.g. [62], the velocity field can only be interpolated about 100 m. Reflecting waves in estuaries also alter the flow speeds by changing the phase, which results in current speeds that do not follow a sinusoidal pattern or is out of phase with the tidal wave (see Figure 1). The variability of tides and effects of tidal phase will be further discussed in Sections 2.5 and 2.6 respectively.

Weather effects such as variations in air pressure or strong winds creating surface waves also affect the flow pattern [60]. Additionally, the drag force induced by wind stress, that is proportional to the square of the wind speed, can push the water on or off shore and alter the sea level and consequently the tidal currents.

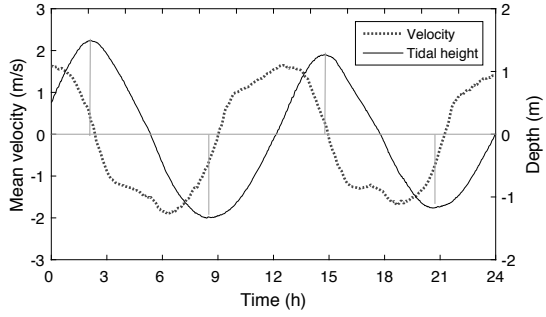

Figure 1. Illustration of the phase shift between tidal height (solid line) and current velocity (dotted line) at the sill of a fjord inlet.

2.3 Turbine wake effects

A marine current turbine that operates in a flow extracts energy from the flow which reduces the velocity behind the turbine. The reduction of flow speed downstream of a turbine compared to the undisturbed flow upstream of the turbine, v_{norm}, is called speed deficit, v_{def}, [63] and is defined as

$$v_{def} = 1 - v_{norm} \quad \text{(Eq. 3)}$$

Generally the wake structure can be divided as near wake and far wake. In the near wake, the flow speed is decreased since momentum is extracted and since mass is conserved the wake expands during the first diameter (D) behind the turbine. The turning turbine blades and the support structure introduces vortices in and around the wake. Typically, the near wake reaches up to 3D–4D [63]. The wake convects downstream where it is exposed to turbulent mixing. Thus, the wake takes up energy and expands at the same time. This effect is prevailing in the far wake. Far downstream, the velocity is restored to that of the incoming flow.

Marine turbulence, affecting the wake propagation, is mainly produced at the boundaries at shallow sites: the seabed and the surface. The seabed creates a boundary layer which strength is dependent on material and bathymetry. The boundary layer is turbulent and affects the velocity profile. At the surface, waves and swell cause turbulence and circular motions. [63]

The wake effect behind turbines has been studied mainly with numerical models and scale models [64–66]. Reports of in-field measurements of wakes from vertical axis turbines seem to be lacking. Thus, the aim of the investigation in Paper IV was to perform in-field measurements of the wake behind the vertical axis marine current turbine in Söderfors. Then an evaluation was performed of the survey and data processing methods, and a first indication of the extent and characteristics of the wake was shown.

2.4 Cavitation-induced flow

In-stream energy converters placed in channels or narrow straits between islands, may be affected by boat traffic. When a vessel travel through water, its propeller or water jet produces turbulence in its wake. Propellers also produces distinct blade tip vortices. The wake is to a large extent due to cavitation, as well as friction between the boat hull and surrounding water.

Cavitation in water is due to the formation of vapor cavities, i.e. small bubbles filled with vapor. This occurs if the pressure decreases below vapor pressure due to high local flow velocities. The bubbles expand, and when the pressure increases above vapor pressure again, the bubbles implode causing an intense shock wave [67,68]. If the shock wave is released close to a solid surface, it may lead to significant damage. Cavitation-induced flow may disturb the flow that propels a turbine, and thus affect the aerodynamic properties of, and loading on, the turbine blades. The turbulent wake is not only constrained to the surface, its effect may propagate downwards into the water column.

Wakes may be observed with ADCPs when the main concern is the velocity fluctuations or deficits (as in Paper IV). However, in Paper V, the aim was to investigate the depth extent and geometry of the cavitation-induced flow in the wake of transiting vessels, as well as compare the effect of different thrust mechanisms (propeller or water jet). The investigation was conducted with two sonar systems (presented in Section 3.2). The extent of the wake, both in space and time, may be measured with a sonar due to the presence of bubbles, as shown in e.g. [69].

2.5 Variability of renewable resources

The renewable energy that may be harvested from wind, solar, wave and tidal resources are variable (intermittent) and non-dispatchable, meaning that the energy content varies with time and cannot be planned in the same way as for other renewable sources (hydropower, geothermal heat and bioenergy). The intermittent renewable energy (IRE) sources have a great potential worldwide to generate large amounts of electricity. For example, wind power generated 42% of the electricity demand in Denmark in 2015 [4] and prices falls continuously. Recently, solar power was proven to have the capacity to be cheaper than fossil fuels. However, integrating the IRE sources into the existing electricity grid will introduce a higher level of variability at the grid and thus increase the need for reserve power and balancing costs [70].

Paper VI presents a review of previous research on temporal variability assessment and forecasting methods for solar, wind, wave and tidal power. The different research areas are at different stages and previous studies have typically covered each resource separately (e.g. tidal energy in Ireland [71]) whereas in a future energy mix, all of these sources will be present. A few

exceptions are studies where tidal power has been combined with wave power [70] and a study combining wind and solar power [72], both performed in the UK. A study from the US of a future scenario with 100% renewable energy takes all of the sources into account [73].

The spatial and temporal variability of the four resources was characterized in Paper VI. Here follows an overview. Wind energy increases towards the poles due to the driving mechanism of large scale flow patterns. Wind speeds and thus wind power generation is higher during winter than summer. The wind blows all day around, in the larger scale it depends on mesoscale weather phenomenon, and on the local scale of topography, surface roughness and thus turbulence. The conditions are highly site specific. Wind speeds are highly stochastic, so the variation is profound on small time scales.

Solar energy varies with the amount of incoming solar irradiation at a site. The solar radiation is higher closer to the equator and lower towards the poles. The seasonal effect variation is due to the solar height which also affect the energy content. Daily variations include larger radiation in the middle of the day, whereas at night it is zero. Tilting the solar panels increases the inflow. The presence of clouds decreases the solar energy compared to clear-sky conditions and may cause the power to ramp up or down, as will shadows from obstacles.

Wave power varies due to the variation of wave heights, which is driven by the wind. The variations are small over relatively large areas. A higher seasonal variation is found in the northern hemisphere than in the southern. The variation in wave height depends on the site, some have generally high waves while others experience a large range.

Tidal energy has a clear temporal variability and is geographically constricted to certain areas where the tidal wave causes high tidal currents, as discussed in Section 2.2. The temporal variability is characterized by three main factors: the tidal regime (semidiurnal or diurnal ebb/flood), the tidal cycle (spring/neap tides) and effects due to site bathymetry (asymmetry between ebb and flood, turbulence, phasing). Spatially, the timing of peak tidal currents differs between sites due to the phase shift that occurs when the tidal wave propagates across a larger geographic area. Also small variations within a site may occur. The predictability of tides is an advantage when planning the electricity availability, as is the phase shift between sites that can be used to smooth out the power production when a number of sites are aggregated.

As discussed in Paper VI several studies have concluded that aggregating power plants in a larger geographic area will lower the variability in power output for all of the IRE sources. For wind and solar power the effect of passing weather systems and clouds will then be smoothed out. For tidal power, aggregation of tidal farms with different tidal phase will give a smoothing effect. Even local phasing at a single site has been suggested to give a smoothing effect [74]. It is also possible to decrease the rated power of each device to increase the capacity factor [75].

2.6 Tidal phasing and aggregated tidal power

As discussed above, tidal power varies continuously between peak values and minimum values up to four times a day, a variability that is generally not preferable when integrated at the electricity grid. To minimize this variability, one solution is to aggregate tidal power from numerous sites, with complementing tidal phase (time lag), to decrease the variability. This has earlier been investigated for a larger region [34,76–78], in a single fjord system [74] or tidal strait [31] for example.

In Paper VIII, the possibility to aggregate tidal energy sites along the Norwegian coast was investigated. The 2500 km long Norwegian coast offers numerous possible tidal energy sites in the fjords where the tidal currents are accelerated. The tide ranges from 0.5 m in the south to 2.5 m in the north and progresses northward along the coast– resulting in a large time lag between south and north. The time lag generally increases northward, with largest time lag in the far northeast. The tidal current resource in Norway is reviewed in [59].

The phase shift between sites may be used to lower the variability. A complementing time lag means that signals that are out of phase will act smoothing on the resultant signal. Two sites that are totally out of phase have a time lag of ¼ of a tidal cycle, i.e. ~3 hours.

Calculating the energy resource with the flux method will overestimate the resource [5,9]. The extractable energy at a site is only a fraction of the incoming kinetic energy. It depends on many things such as number of installed devices, packing density, blockage ratio, efficiency of the farm etc. To take all of this into account Black & Veatch [79] suggested that the extracted energy should not exceed a significant impact factor (SIF) and it is the percentage of available energy that can be extracted from a flow without significantly changing its properties. According to [79], SIF may have a value of 10%–50% depending on the site. It was said to be 20% on average in the UK [80]. The theory was supported by [81,82]. This method was used in Paper VIII as described in Section 4.3.2.

3. Instrumentation

A large part of this work is based on field measurements of hydrological phenomenon such as tidal currents and turbine wake characteristics. In this work, two types of instruments have been used, which are presented below.

3.1 ADCP: Acoustic Doppler Current Profiler

The instrument used for measuring current velocity is an acoustic Doppler current profiler (ADCP) from Teledyne RD Instruments of the type Workhorse Sentinel ADCP of 600 kHz[3]. The instrument transmits acoustic pulses from four transducers at a certain frequency and interval. The sound pulses are sent out in bursts of a number of pings and reflect on particles in the water. The Doppler shift in the frequency of the returning signal is used to calculate the flow speed. The time it takes for the signal to return corresponds to the distance from the transducer head to the middle of the depth cell. The obtained velocity profiles give information on the flow velocity along the four beams of equally spaced depth cells. The beam velocities are transformed to earth coordinates by the instrument giving the output as north (u), east (v) and vertical (w) velocity so that $U = (u, v, w)$.

The transducers are separated by an angle of 20° from the centerline of the ADCP. Thus, the distance between the beams is increasing with depth, see Figure 2.

[3]http://www.teledynemarine.com/workhorse-sentinel-adcp/?BrandID=16 (2017-02-16)

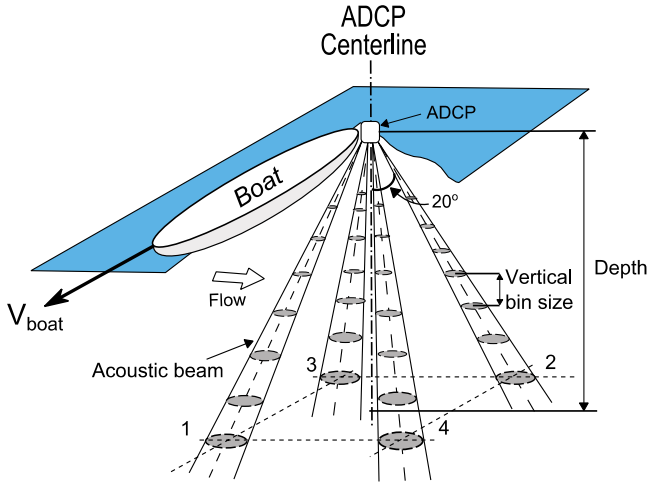

Figure 2. Sketch of ADCP operating in upside down mode from a boat.

The ADCP assumes a horizontally homogenous velocity field when calculating the water velocity from three (or four) beams. Thus, any small scale turbulence is averaged out. For an observation to be of good quality, at least three good quality beams, i.e. beams with high correlation, are required in the solution. The fourth beam is to ensure better quality. For each burst of N pings, an ensemble average is calculated by the instrument. The Doppler noise uncertainty can be large but is decreased by a factor $1/\sqrt{N}$.

Built-in sensors give information on the physical status of the ADCP. A pressure sensor provides the depth at the transducer, a compass gives the heading and a tilt sensor gives information about the tilt of the ADCP (pitch angle and roll angle depending on around which axis the tilt occurs).

When used in the upside down mode, an extra Bottom Tracking pulse can be transmitted. It has a longer wave length and tracks the speed of the bottom with high accuracy.

3.2 Sonar: Multi-beam and dual beam

The turbulent wakes of transiting boats were observed with two sonar systems, a multi-beam sonar (MBS) system and a dual-beam sonar (DBS) system (Paper V). As with ADCPs, a sonar is an echo-ranging technology. The term SONAR stands for Sound Navigation and Ranging. Active sonars transmit acoustic signals and use the received echo to get an underwater view of the bottom and locate targets within a water column, often in a wide angle around the instrument.

The energy and propagation of the sound pulse are affected by a number of parameters. The speed depends on water temperature. Acoustic intensity is the mean energy flux per area and time. The sound pulse is affected by absorption, mainly due to the viscosity of the water. The absorption depends on the frequency of the sound; higher frequencies are dampened more. Moreover, the signal is exposed to losses at the surface and bottom due to reflection and scattering. The geometric spreading due to expansion is spherical and occurs twice, both for the transmitted signal and the reflected echo [83].

A multi-beam sonar system consists of an array of transducers that transmits sound pulses in several directions simultaneously in a fan shape that provides data along a wide swath of the studied area (e.g. the seafloor). The swath is oriented perpendicular to the center of the instrument. The field of view (FOV) of the sonar is expressed as the maximum angle, horizontally and vertically. The echo of each sound pulse is processed separately and gives information of the distance to the reflecting object within the swath. The range is limited to 100 m. The system is subject to disturbance from e.g. background noise and noise due to bubbles, which on the other hand can be used to study cavitation-induced turbulence. The MBS used in Paper V has 768 beams separated by 0.28°, an operating frequency of 900 kHz and a FOV of 130° horizontal × 20° vertical (Paper V).

A dual-beam sonar system transmits two cone shaped single frequency signals, one narrow and one wide. The narrow core beam has a higher frequency and gives a more detailed image while the wider signal has a lower frequency and covers a larger area. DBS systems only measures acoustic intensity or amplitude, not the phase of the signal [84]. The DBS used in Paper V operates at the two frequencies 50/200 kHz with a FOV of 29°/12° respectively.

A general sketch of two systems are shown in Figure 3.

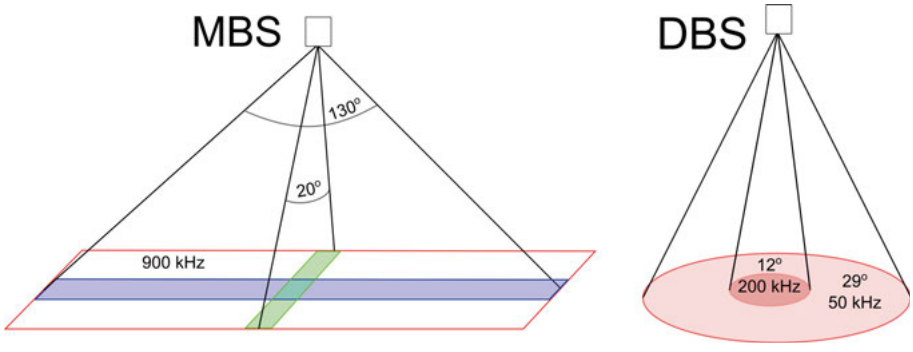

Figure 3. Sonar beam spreading from the multi beam sonar (MBS) and dual beam sonar (DBS) systems used in Paper V.

4. Methods

4.1 Resource assessment methodology

In this section, resource assessment methods will be discussed from a tidal energy point of view, with focus on methods used within the scope of this thesis.

4.1.1 Site selection

When searching for a site with potential for in-stream tidal energy conversion, an area where the flow is constricted in some way, and thus accelerated, is favorable. The higher the flow speed, the more available energy (Eq. 1). For developers of marine current energy converters of the first generation, flow speeds exceeding 2 m/s and depths of about 20-50 m are required. For 2nd and 3rd generation turbines, where lower velocities and shallower sites also are of interest [15], the number of potential sites around the world is increased.

The first step taken in a resource assessment survey is to locate a site with sufficient depth and water speeds. Ship navigation charts (e.g. [85] in Norway) may be used as initial source of information. Potential sites can also be found by analyzing nautical charts. Areas to look for are, for example, narrow and shallow fjord inlets in areas with tides and a large enough basin inside the sill where sufficient flow speeds, with a high energy content, may occur. Straits between islands may be even better at providing high currents where extraction of energy will not affect the flow as much as in a constricted channel. Areas where the flow accelerates around a headland or peninsula are also advantageous for tidal energy conversion.

Apart from high currents and sufficient depth, project planners also need to consider bottom structure (how to place the turbines), vicinity of houses and possibilities for grid connection, as well as the interference with other interests such as boat traffic and wild life.

The second step is to choose measurement method. Normally, this is done by first performing a transect measurement survey to conclude whether the site has sufficient water speeds ($>$ 1 m/s) and if so, map the spatial variability at the site. Often, the most energetic area is investigated further through long-term measurements of current speeds.

4.1.2 ADCP configuration

Each measurement survey needs to be carefully planned in advance. The instrument needs to be calibrated and configured according to the chosen measurement method and the characteristics of interest. Software packages provided by Teledyne RDI are used to "talk" to the instrument (for example BBTalk or PlanADCP). The compass needs to be calibrated in advance of each measurement survey [86].

The ADCP can either be run in real-time mode by keeping it connected to the computer during the measurements, or operate self-contained by programming it in advance and connecting it to one or more batteries. The user needs to consider the required measurement accuracy when setting up the ADCP. In a self-contained deployment, the power consumption is dependent on the measurement intervals and number of pings in each measurement.

The parameters that need to be set by the user are

- Ensemble interval
- Pings per ensemble (N)
- Time between pings
- Vertical bin size
- Number of vertical bins
- Bottom tracking (and depth range)

4.1.3 Transect measurements

To investigate the spatial variance of a flow stream in a watercourse (river or tidal strait), a common way is to measure the velocity profile in cross-sections, along transects perpendicular to the flow direction. The ADCP is then mounted upside down in a floating vessel, Riverboat[4] (Figure 4), and towed across the watercourse with a small boat navigated with help of a GPS (Global Positioning System) as in Papers I and II, or by following leading lines marked at the shoreline, as in Paper IV.

The ADCP can then be configured with the software VmDas and measurement data is monitored in real-time through the software WinADCP provided by the manufacturer. The inbuilt function Bottom Tracking records the speed of the ADCP relative to the sea- or riverbed, and subtracts this speed from the flow speed measurements, to account for the boat motion.

A Garmin EchoMAP 50s has been used to log the GPS-positions during the transect measurements. It has also been used with an echo sounder to investigate the bathymetry (as in Paper I).

[4] Oceanscience Riverboat, http://www.oceanscience.com/products/tethered-boats/riverboat.aspx <2015-11-05>

When high accuracy position data was required (for the wake measurements, Paper IV, see Section 4.2.2) a Global Navigation Satellite System (GNSS) receiver was mounted on top of the ADCP (seen in Figure 4). The Real Time Kinematic (RTK) technique used gives a precision down to 1 cm.

Figure 4. ADCP mounted upside-down in a Riverboat with a GNSS reciever mounted on top.

4.1.4 Long-term measurements

To get the temporal variation of flow speeds at a site, the ADCP can be mounted in a foundation and placed on the seabed (or bottom of the river). Foundations designed at Uppsala University are used for deployments. The foundations are made of stainless steel and weigh about 10 kg (Figure 5). The ADCP is screwed to the bottom plate of the foundation to stay steady. Ballast

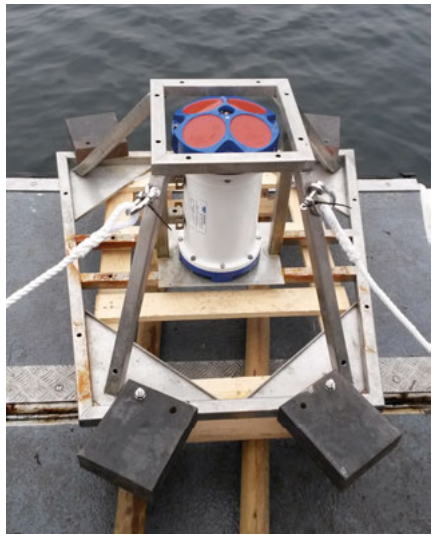

Figure 5. Photo of ADCP mounted in the foundation and ballasted with four weights.

weights of 10 kg each are attached onto the foundation with screws. This was either done in advance in the boat, or by divers at the seabed.

It is important that the ADCP is placed steadily and horizontally on the bottom with minimum tilt (pitch and roll) to ensure good accuracy. The practical aspects of deployment of an ADCP for long-term measurements need to be well planned in advance. The depth of the site determines the length of the ropes used when lowering the instrument and when marking it with a buoy. The expected flow speeds affect the required ballast weight.

4.1.5 Data analysis

The output data from the ADCP, describing the flow characteristics, include flow velocity profiles (north-, east- and vertical components) and flow direction for each depth cell, together with vectors of depth (either from the bottom tracking feature or from pressure) and time (year, month, day, hour, minute, second, hundredths of second). A number of data quality parameters are also given for each observation including (but not limited to):

- Error velocity
- Percent good (PG1-PG4)
- Correlation between beams
- Echo intensity
- Heading
- Pitch and roll

The analysis of ADCP data starts with a quality screening. First observations marked 'bad' by the ADCP, shown as spikes, are removed. Observations where the sum of the parameters PG1 (percent of observations of good quality three beam measurements) and PG4 (percent of observations of good quality four beam solutions) are at least 75% are kept, corresponding to measurements where at least 75% of the pings in the ensemble come from three or more good beams[5]. The error velocity indicates the standard deviation of the horizontal velocity measurement within each bin in each ensemble. It is a key quality parameter that can be used to decide which data points are of bad quality. The error velocity should be less than 1 m/s and the average correlation between beams at least 64 counts (out of a maximum of 255 counts due to a scaling of the signal to noise ratio [87]) . Data close to the seabed or surface (depending on whether measurements are performed downwards or upwards) are interfered with noise and are therefore removed according to $noise = h \cos \alpha$ where $\alpha = 20°$ for the ADCPs used [87].

Heading, pitch and roll angles give information about how steady the ADCP has been during the measurements. That information can be used to

[5] Teledyne RD Instruments, Glossary of Terms <2016-12-19>

analyze whether the instrument has been moved during the deployment, due to strong currents or other external forces. A large movement may have changed the location or tilt angle, inducing measurement errors.

When the data have been quality checked, there are many aspects of the flow characteristics that can be studied (as mentioned in Section 2.1). One approach is to calculate standardized, characterization metrics that can be compared to other sites, as in Paper II. Among these (as proposed by [88]) are mean speed, maximum sustained speed for 10 minutes ebb/flood asymmetry and vertical shear describing the velocity field. Other metrics are principal axis, standard deviation from the principal axis and ebb/flood direction asymmetry describing the directionality ([15,16,32–35]) together with mean power density and ebb/flow power asymmetry describing the energy content ([15,36]). All of these metrics are calculated at expected turbine hub height, which has been proposed to be in the middle of the water column [82]. A vertical profile plot allows for interpolation of the speeds from hub height to other parts of the water column. Such interpolation is often used to calculate the speed at different parts of the turbine sweeping area.

Principal component analysis can be used to study tidal flow directions. The velocity vectors are rotated so that the major principal axis defines the main orientation of the flow, e.g. along-shore, while the minor axis then defines the cross-shore direction of the flow for example. Most of the variance is then associated with a major axis and the remaining variance with a minor axis [89].

It is also of importance to analyze the speed frequency distribution (or probability) for a typical month or for a year. This will affect the amount of energy that a tidal turbine (or farm) can produce depending on its power curve and power capacity. An understanding of the weather effect on tidal range, and thus current speed, at a site may be important for a full resource characterization [37–40]. Weather effects may be substantial, especially at high latitudes where travelling low pressure systems are common during parts of the year. Tidal constituents can be analyzed with harmonic analysis, as in the Matlab toolbox T_TIDE developed by , which also separates tidal from non-tidal components of the signal [90].

For transect measurements it is common to divide the transects into smaller horizontal bins and analyze the data that fall into each bin (also called block-averaging). The assumption is then that data being considered in each bin are statistically homogenous. This technique was used in Paper I to form mean values and time series for a specific part of the surveyed site. However, using sparse measurements to interpolate the flow field can usually not be done with adequate accuracy. To visualize spatial data, maps are a powerful tool.

The variability of a velocity time series may be analyzed with statistical measures such as standard deviation, variance and correlation, discussed further in Section 4.3.

4.1.6 Simple prediction model

A simple model is proposed for the tidal site (discussed in Section 4.2.1) where peak current speeds can be predicted from tidal chart data in a tidal strait connecting the ocean to a fjord. A linear relationship is assumed between tidal range and peak current speed, U_{max}. When the linear relationship is found, the model allows readily available tidal elevation data to be used to predict long time series of peak current speed. This is done in Paper II.

The model is set up in a number of steps. First, tidal chart data, often given as an interpolated value from nearest gauge station, is calibrated to the site specific tidal range. The tidal range, H, is calculated as the difference between each high and low tide and vice versa. Then, predicted tidal range is compared to measured tidal range to ensure a small deviation. At last, the linear relationship (slope and y-intercept of the linear regression) is established between measured tidal range and peak current speed.

The model accuracy is estimated from the standard deviation in U_{max} for increments of 0.2 m tidal range. Weather effects on tidal range and thus current speed are quantified. The model is evaluated for two other heights above the seabed, and at expected hub height. Also the effect on the model of a shorter measurement period is investigated to find the shortest possible measurement period. The correlation coefficient between measured tidal range and peak speed has been analyzed as well as the slope and y-intercept from the linear regression.

4.2 Field work

4.2.1 Tidal site: Korsnesstraumen

Potential tidal energy sites are numerous along the coast of Norway due to the large number of fjords. The tidal height in Norway reaches from about 0.5 m in the south up to a maximum of 2.5 m in the north [91]. The tidal site that has been investigated is located in the Folda Fjord, in Korsnesstraumen at the sill to its inner part, Innerfolda (see map in Figure 6).

Two measurement surveys were conducted at the site. The initial spatial mapping of the speed variance and expected maximum velocities are presented in Paper I. From these results, the most energetic area was chosen and long-term measurements were planned and performed during the year after, see Paper II.

Four transects were investigated during the initial survey in August 2013 (Figure 6). Each transect was covered three times during flood and three times during ebb by towing an ADCP along the surface with a boat (Figure 7). The measurements were performed in tracks from west to east then back again.

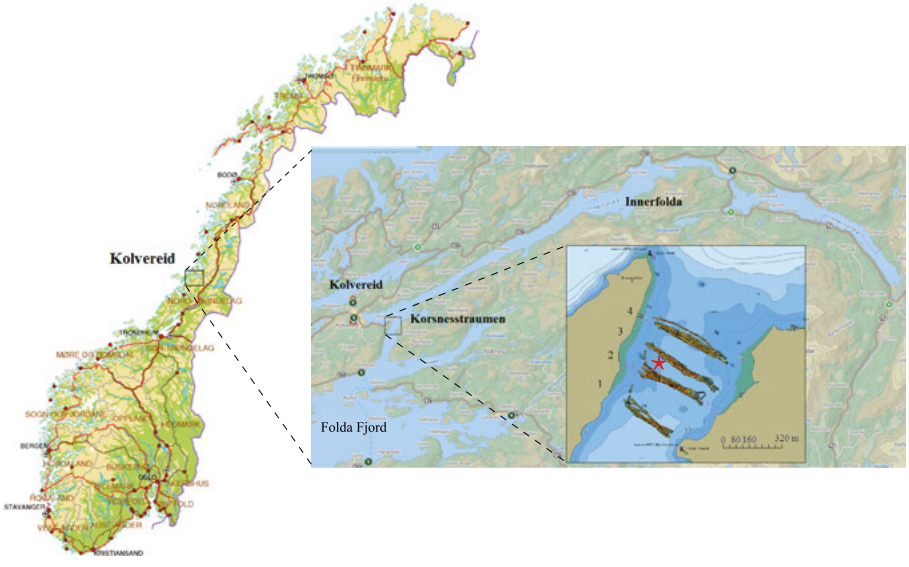

Figure 6. Overview map of Norway and in detail over the inner part of the Folda Fjord and Korsnesstraumen. Measurements in Transect 1-4 are shown. The star marks the location of ADCP deployment.

Each track took about 10 minutes to complete. The tidal currents were assumed to be constant during the completion of one track. For each track, horizontal bins of about 50x50 meters were defined and the depth averaged speed within that area was calculated. An area in the western part of the fjord inlet, between Transects 2 and 3, was chosen for further investigation due to its uniformly high speeds during ebb and its high peak speeds during flood.

Figure 7. During the transect measurements, the ADCP was mounted in a RiverBoat and towed across the stream.

The ADCP was deployed for long-term measurements in June 2014 with assistance of a team of scuba divers who secured it horizontally at the seabed and then mounted the 60 kg of ballast on the foundation. The ADCP was recovered later on, in August, after 54 days of measurements.

4.2.2 River site: Dalälven Söderfors

A marine current energy converter was deployed in March 2013 at the river site in Dalälven in Söderfors, as described in Paper III (see Figure 8). Simultaneously, three ADCPs were deployed: one upstream of the bridge to monitor the incoming flow, one on the middle bridge pillar that measures horizontally and one downstream of the converter (see Paper III Fig. 3). The turbine has 5 blades with a height of 3.5 m and a turbine diameter of 6 m. It is mounted on a generator which is then attached to a tripod foundation (for design, see Paper III Fig. 5). Since the deployment, the control system has been tested and improved so that the system can be operated in flows from about 0.6 m/s, at different rotational speeds (Paper IV).

The wake behind the converter was investigated in Paper IV for a case when the turbine was rotating at a tip speed ratio of approximately 5.6. Meas-

Figure 8. Photo from the deployment of the turbine in Söderfors.

urements of vertical velocity profiles were performed across and along the flow by slowly towing an ADCP behind a small boat to get cross-sections of the flow speed. Leading lines were established on shore to ensure that the measurements were performed at the same location each time. The ADCP was set up to measure 5 pings/ensemble with 1 Hz sample frequency.

4.2.3 Ocean current site: Finnhamn

Two measurement surveys were conducted to investigate a possible high energy current site in the Stockholm archipelago. High currents had been experienced in a sound between two islands east of the island Finnhamn. Finnhamn is mainly used for tourism and recreation with year round activities and would benefit from a local renewable energy production.

The tide in the area is negligible, so the currents were assumed to be ocean currents, either thermally induced, due to pressure and wind or fresh-water runoff from the mainland. The surveys had two aims: to map the current velocity and to study the wake effects of some of the ships that transit the area. The study is also reported in [92].

The first survey was conducted on November 20, 2014. Water current velocities were measured with an ADCP in cross-sectional transects and in transects along the flow. Simultaneously, two sonar systems studied the seafloor and the wake effects from ships of opportunity (which will be discussed below).

In Figure 9, mean current speeds are plotted where they were collected across and along the flow. From those measurements, two areas were strategically selected for long-term measurements: one in the southern end of the sound (A1) and one in the northern (A2).

For the second survey, two ADCPs were deployed at the seabed in the two selected areas. Measurements were performed for about a month between December 17, 2014 and January 29, 2015. Information about the long-term measurements is seen in Table 1. Data were collected at a rate of 1 ping/s for 30 seconds each minute. Flow speeds were analyzed for 30 second ensemble mean values and 10 minute mean values. The measured speeds are presented for expected turbine hub height, i.e. the middle of the water column.

Table 1. Information from long-term measurements of ocean currents with two ADCPs.

	ADCP 1	**ADCP 2**
Number of days	43 days	44 days
Coordinates	59.47898°N, 18.82937°E	59.48312°N, 18.82804°E
Mean depth	13.2 m	22.1 m
Expected hub height	6 m	11 m

The current speeds measured during the first survey were slow, in the range 0 – 0.6 m/s, in the 0.5 m depth bin corresponding to about 6 m from the surface. Also the long-term measurements show low mean speeds, ~ 0.1 m/s, and maximum speeds of less than 0.7 m/s for both sites (A1 and A2). The direction of the flow follow the sound and are thus mainly northwesterly and southeasterly.

From these results, the site was considered to not have potential for energy conversion. Thus, no further discussion of the results will follow.

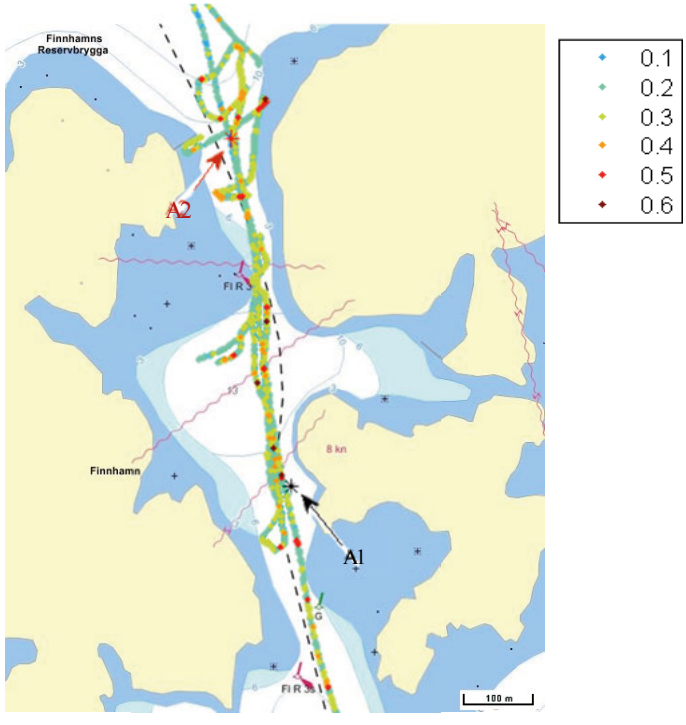

Figure 9. Mean speed from transect measurements, calculated at the depth 5.5-6.5 m (from the surface). Mean speed is given by colors (in m/s). The areas for deployment of the two ADCPs, A1 and A2, are marked with stars [92].

The seafloor bathymetry was imaged and wake effects from ships of opportunity were studied during the first survey. The two sonar systems, the MBS system and DBS system (Section 3.2), were attached to the side of the boat using a pole mount and had their transducer heads at 0.5 m depth. The MBS transducer head was tilted 45° compared to the water surface whereas the DBS was headed perpendicular to the water surface. A GPS simultaneously measured the positions. The MBS system may measure from a distance, since it is tilted, whereas the DBS system measures straight down and thus needs to be placed above the flow that is due for investigation.

Two different types of vessel thrusters were studied: propeller and water jet driven engines. The survey boat parked near point A2 (Figure 9) from where it was possible to get an underwater view of the wakes of the passing ferries. The two observed ferries were M/S Värmdö with a propeller thruster, and M/S Cinderella I with a water jet thruster (for technical specifications see Paper V Table 1).

4.3 Assessment of renewable energy variability

4.3.1 Combining solar, wind, wave and tidal energy in the Nordic countries

The effect of integrating a higher share of IRE (intermittent renewable energy as defined in Section 2.5) into the Nordic power system is investigated in Paper VII. The aim was to find out for which time scales variability is of largest concern and whether a wise combination of intermittent renewable energy sources may reduce the variability. Thus, the net load was analyzed by separating the variability into different frequency bands to determine which mix of renewables that is optimal for reducing the variability on different time scales.

Each of the intermittent renewable resources (wind, solar, wave and tidal) were modeled in terms of time series of hourly values of generated energy (TWh/h). This was done for a number of power plants across the Nordic countries (Norway, Sweden, Finland and eastern Denmark), with solar and wind power concentrated to Sweden and wave and tidal power concentrated to the Norwegian coast (see Paper VII Fig. 1).

The sources were first analyzed one by one for a production limited to 3 TWh/year each (which was also the maximum production of the tidal farms in the study). Then the 3 TWh/year limit was removed and the sources were combined in two scenarios.

Each of the energy time series were then analyzed on different time scales by separating them into four frequency components: long-term (LT), mid-term (MT), mid/short-term (MST) and short-term (ST) components. The importance for analyzing long-term variations is the seasonal storage capacity of hydropower ($>$ 4 months), the mid-term variations (2 weeks to 4 months) corresponds to largest fluctuations in tidal power, the mid/short-term variations (2 days to 2 weeks) corresponds to large fluctuations in wind and wave power while the short-term variations ($<$ 2 days) has a high impact on fast balancing requirements.

To quantify the variability the step change (difference in power from one hour to the next) was calculated. Furthermore, the standard deviations of each source for the different frequency components were compared.

Two scenarios were investigated. The "highly renewable scenario" where fossil energy, old IRE and 30% of the nuclear energy were replaced by new IRE (from wind, solar, wave and tidal power systems) with a total of 72 TWh/year which then accounts for 20% of the total load in the system. In the "fully renewable scenario", all fossil energy, old IRE and nuclear energy were replaced, resulting in 36% new IRE, which corresponds to ~130 TWh.

For each scenario two reference combinations were investigated. Mix 1 is similar to today with 90% wind and 10% solar energy. Mix 2 is more futuristic with maximum tidal energy (3 TWh/year) and the remaining divided as 40% wind, 40% solar and 20% wave.

The mixes were then optimized to reduce the net load standard deviations for each frequency component ($\sigma_{LT}, \sigma_{MT}, \sigma_{MST}, \sigma_{ST}$) and the total standard deviation for the raw data (σ_{raw}) according to Eq. 4.

$$\sigma_{raw} = \sqrt{\sigma_{LT}^2 + \sigma_{MT}^2 + \sigma_{MST}^2 + \sigma_{ST}^2} \qquad \text{(Eq. 4)}$$

4.3.2 Aggregating tidal energy in Norway

For tidal energy, it is possible to take advantage of the phase shift that occurs when the tidal wave travels the long distance along the Norwegian coast. By aggregating a number of tidal sites with different time lags, a smoothing effect occurs in the short-term component due to the phase lag between sites.

In Papers VII and VIII, 114 sites from south to north were studied, with a relative time lag of up to 6 hours. To analyze the variability, a power production model was set up based on [29,59]. However, accurate tidal current velocity data is sparse or non-existing in this area. Instead, information on tidal currents was extracted from pilot books ([85,93–95]) that describe the current strength at numerous sites. These descriptions are interpreted as the average peak spring speed at the site. The time lag was extracted from tidal charts for each site and site width and depth were extracted from electronic nautical charts online.

A few assumptions are made to turn the velocity data into a velocity time series with correct properties that match the semidiurnal tide. A sinusoidal signal was applied and then altered by applying area specific coefficients (see Paper VIII Table II). These coefficients determine to what extent the flood tide is smaller than the ebb tide, that the second tide each day is smaller than the first, that neap is smaller than spring and that the second spring each month is smaller than the first spring.

A time lag was added to each time series to create the phase shift between the sites. Since tidal constituents for each site were unavailable during this work, the model was set up in discrete time steps (of 1 min). The flux method was then applied to calculate the available power density at each site. No certain turbine or farm layout was chosen, instead only a fraction of the energy

was extracted by applying a significant impact factor (SIF) (cf. Section 2.6). Thus, SIF can be seen as a constant conversion rate. For the sites in this study, SIF has been varied from 5% to 20% of the incoming kinetic energy. The resulting time series is produced energy in 10 min time steps (Wh/10 min). These are used in Paper VIII to investigate the variability in the total available tidal energy and in three scenarios.

The sites are shown at the map in Figure 10 and their relative time lag is seen in Figure 11. The four most energetic sites are No. 30, 57, 99 and 105 which are marked on the map and seen in Figure 11.

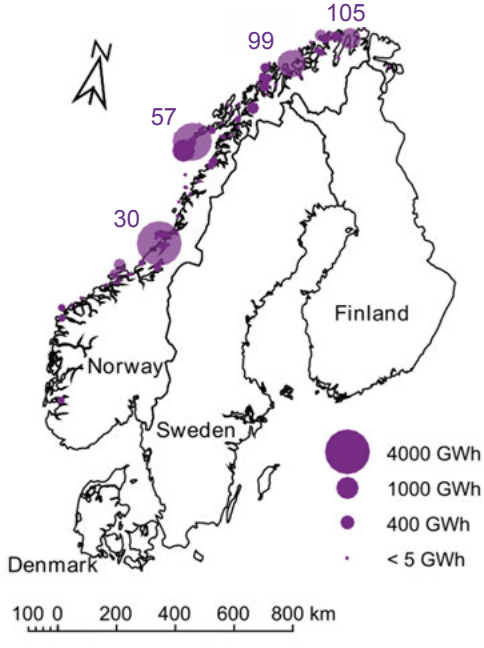

Figure 10. Tidal sites marked at their respective location. Circle size corresponds to available energy at the site (Fig. 2 in Paper VIII).

Three scenarios were investigated where two variables were varied: the number of sites and the fraction of energy extraction (SIF). The scenarios were chosen based on their potential. The sites with the highest potential were assumed to be of most interest for a future exploitation. They were also chosen to include a variety of time lags. In addition to the sites mentioned above, site No. 19, 54 and 112 are part of all Scenarios.

Scenario 1: 7 of the most energetic sites, SIF 20%
Scenario 2: Same 7 sites, varying SIF (5% – 20%)
Scenario 3: A total of 17 sites, varying SIF (5% – 20%)

In all scenarios, the largest time lag is 4.4 hours (between site 19 and 105). In Scenario 1, a constant SIF of 20% is applied to all sites, while in Scenario 2 SIF is varied between 5% and 20% where a smaller fraction of the available energy were extracted at the largest sites – so that a smoothing effect occurs. In Scenario 3, an additional 10 sites were added and SIF was varied in the same manner.

The variability was then quantified through a measure of the standard deviation in each of the four filtered time scales, following the procedure in Paper VII (outlined in Section 4.3.1). Apart from the standard deviation, also the 10 minute step change was analyzed, i.e. the change in energy in 10 minute steps.

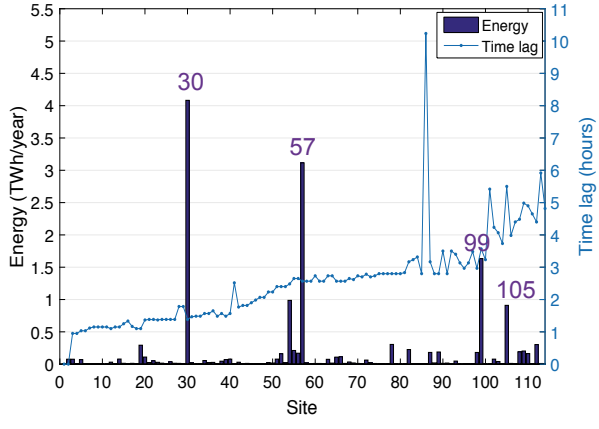

Figure 11. Available energy (TWh/year) at each site numbered from south to north and corresponding time lag in hours (Fig. 3 in Paper VIII).

5. Results and discussion

5.1 Tidal site: Characteristics and resource

The results from the transect measurements in Korsnesstraumen in Paper I are shown in Figure 12 where it is seen that the highest and most uniform speeds are found in the west part of the sound, in the area between Transects 2 and 3. This area was further investigated in Paper II and an additional transect was addressed (Transect 2b) close to where the ADCP then was deployed, as seen in Figure 13.

The resultant time series from the long-term measurements is seen in Figure 14 for current speed at assumed hub height (6.1 m from the seabed). It is seen that the currents do not follow the same strictly sinusoidal pattern as the tide (cf. Figure 1). This confirms that the currents are more unpredictable and require measurements to be characterized properly. The distribution of speeds is seen in Figure 15 for all measurements and for a "typical month", chosen as 7 July – 5 Aug 2014. The mean speed at hub height is the same for flood and ebb, 1.02 m/s, but the maximum speed sustained for 10 min is higher for ebb, 2.06 m/s compared to 1.86 m/s for flood. The cumulative distribution shows that the velocity is more than 0.6 m/s during 72.7% of the time (corresponding to the cut-in speed for the vertical axis turbine in Paper IV), and exceeding 1 m/s for 38% of the time. The measured peak speed was 2.17 m/s.

The vertical profiles in Figure 15 are 10 minute mean values at peak flows for flood and ebb during spring and neap (marked in Figure 14). They show a larger shear in the lowest half of the water column, and rather uniform flow in the upper part. Around hub height, the vertical shear is on average 0.05 m/s per meter for ebb and half of that for flood (see Paper II Table 4).

The channel-like bathymetry of the site results in an almost completely bi-directional flow, which is favorable for most tidal energy converters (see Paper II Fig. 6).

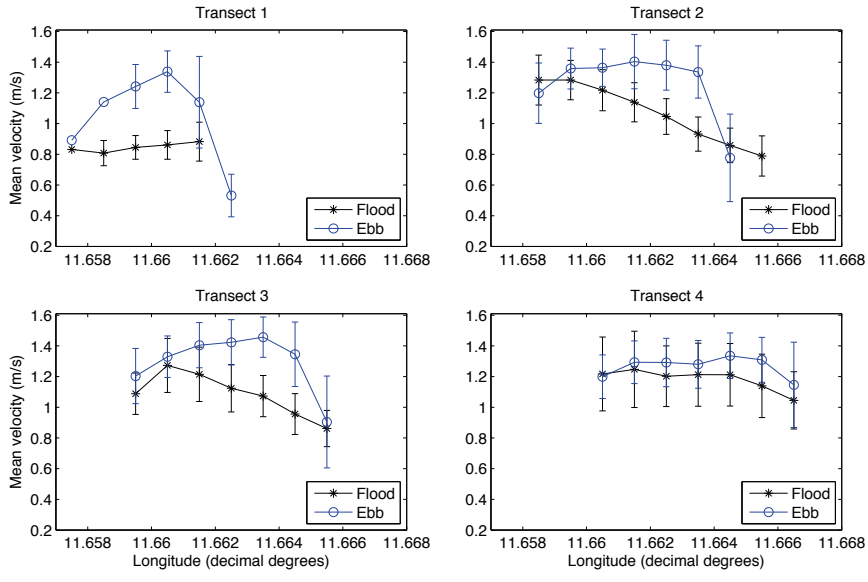

Figure 12. Mean speed and standard deviation for each transect, calculated for horizontal bins, for ebb and flood respectively (Fig. 4 in Paper I).

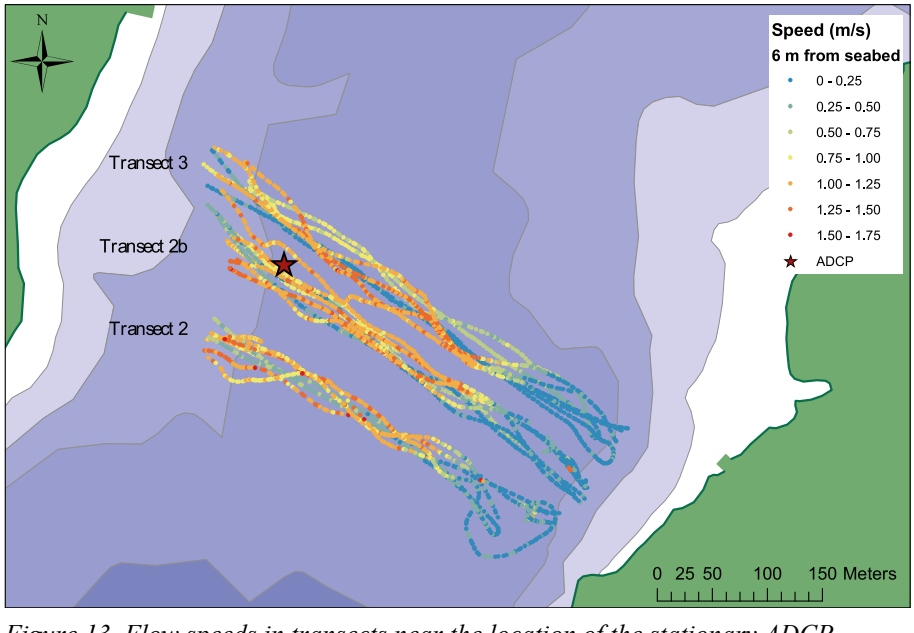

Figure 13. Flow speeds in transects near the location of the stationary ADCP (marked with a star). Bathymetry is shown, where darker shading corresponds to deeper sea (Fig. 15 in Paper II).

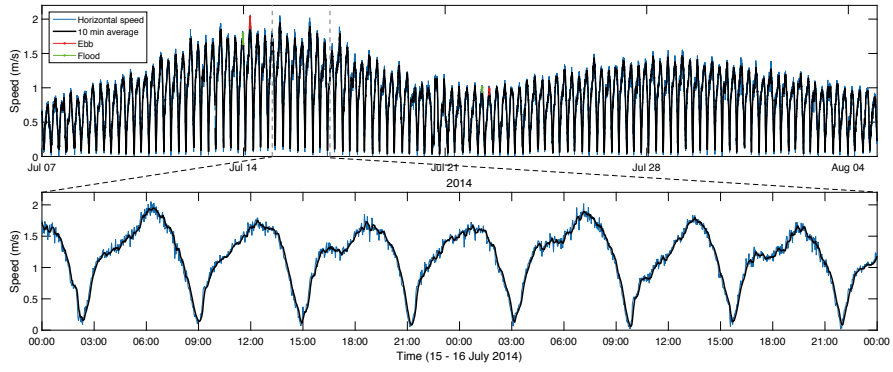

Figure 14. Top: Long-term measurements of tidal current speed at hub height for the entire measurement series. Bottom: Detailed view for 2 days of measurements (from Fig. 3 in Paper II).

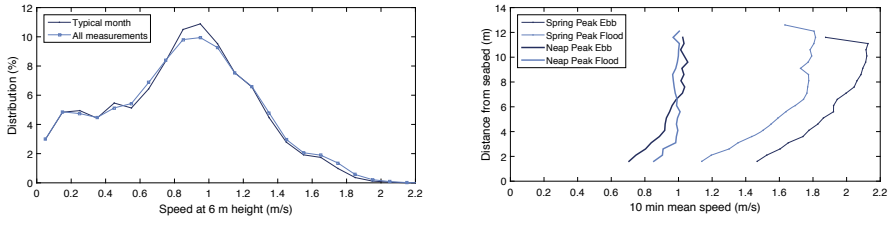

Figure 15. Left: Distribution of measured speed at hub height for all measurements and for a "typical month". Right: Vertical profiles of ebb and flood flows during spring and neap respectively (Figs. 4 and 5 in Paper II).

5.1.1 Simple prediction model

The results from the simple prediction model show that the measured tidal range is typically 3% larger than the predicted but otherwise show a small deviation from the linear relationship. The linear relationship between tidal range and peak current speed (Figure 16) is shown to be strong with a correlation coefficient of 0.98 at assumed hub height (6.1 m), and the standard deviation in the measurements is less than 10 cm/s from the linear relationship given by

$$U_{max} = 0.647H + 0.165\ m/s \qquad \text{(Eq. 5)}$$

The non-tidal effects (of ±30 cm on tidal range) would give ±0.19 m/s difference in peak speed at hub height following the linear relationship (Eq. 5). The maximum expected peak speed is 2.12 m/s at hub height.

The results of the evaluation of varying hub height show that closer to the seabed (3.1 m), where the current peak speeds are lower, the speed variation with height is not as steep as for hub height (6.1 m). Closer to the surface (9.1

m), peak speeds are higher but the linear relationship is similar. Furthermore, the evaluation of the effects of measurement period length shows that at least 9 days of measurements are needed to reach a correlation coefficient of at least 0.9 and reduce the relative error in peak speed to 3%. After 29 days of measurements, the relative error is less than 1%, but the error is expected to vary depending on where in the monthly tidal cycle the survey begins (see Figs. 11 and 12).

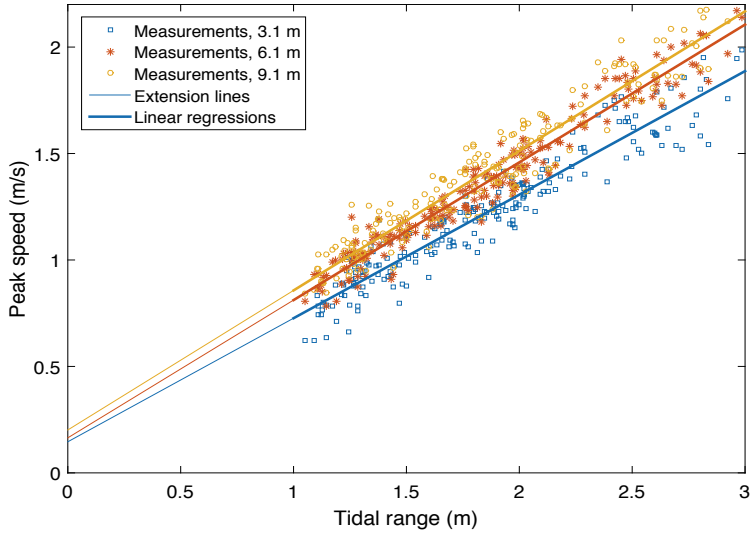

Figure 16. Linear relationship between tidal range and peak speed for three different heights above the seabed (Fig. 10 in Paper II).

These results, although site specific, show that the simple prediction model can be used to predict peak current speed from information on tidal range on this and similar sites, i.e. tidal straits connecting the ocean to a bay or fjord. It is suggested to measure for at least 1/3 of the tidal cycle. If the measurement period is short, it is furthermore suggested to focus on performing measurements around the largest spring tide to make sure to catch both smallest and largest tidal ranges and thus smallest and largest peak speeds.

5.2 River site: Wake effects

Figure 17 shows depth mean speed, i.e. average speed over the entire water column, for several measurement runs downstream of the turbine (marked with a circle), plotted where collected. The depth mean speed, indicated by colors, has been normalized by the undisturbed depth mean speed, as meas-

ured upstream of the turbine. Each grid square corresponds to one turbine diameter. A wake is prominent as an area with higher speed deficit, i.e. lower speeds, behind the turbine. It was seen to extend some 6 to 7 turbine diameters downstream.

To give a more realistic appearance, the transects were projected along straight lines. Figure 18 shows the cross-sectional velocity profiles for three of the across-flow transects (C1, C2 and C3) at 1.3, 5.4 and 9.7 turbine diameters distance downstream, respectively (c.f. Paper IV Figs. 5 and 6). The wake is clearly seen in C1 and C2 downstream the turbine, while in C3 the wake cannot be readily distinguished.

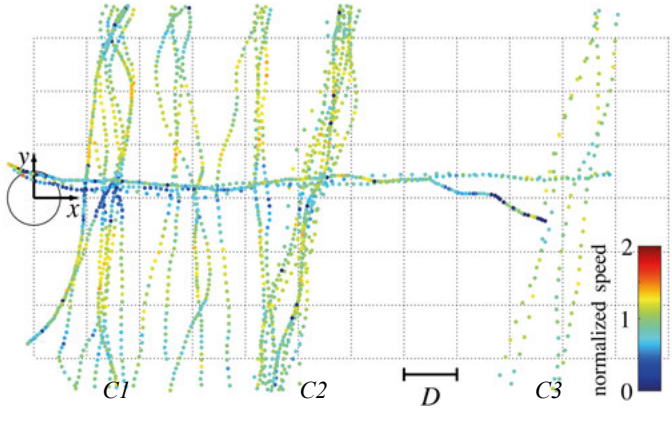

Figure 17. Depth mean speed (in m/s) as measured in transects downstream of the marine current energy converter. Circle denotes the turbine. Each grid square equals one turbine diameter. The wake is visible as lower mean speed (Fig. 7 in Paper IV).

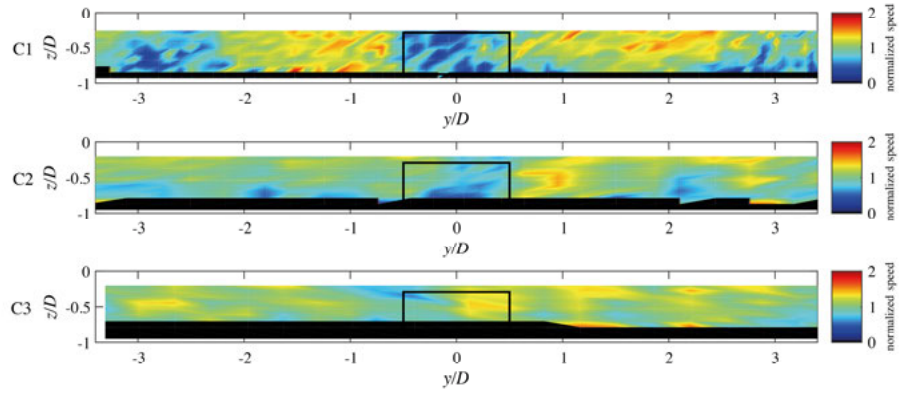

Figure 18. Cross-sectional velocity profiles for three transects at 1.3, 5.4 and 9.7 turbine diameters respectively. The projected turbine swept area is marked with a square (Fig. 9 in Paper IV).

5.3 Ocean current site: Cavitation-induced flow

The results from the sonar measurements of cavitation-induced flow are summarized in Table 2. It is seen that the wake of two different thruster mechanisms takes on different geometry. According to the resulting images from the MBS, the cavitating flow behind the propeller ferry consists of a cloud of bubbles that spreads into a cylindrical shape whereas the water jet wake takes on a conic geometry (see Paper V Fig. 7). The propeller wake reaches further down but has its core density closer to the surface, compared to the water jet. The intensity was higher in the propeller case. On the other hand, so was the background noise. From DBS data it was possible to conclude that the turbulent wake lasted approximately 90 s for both thrusters.

Table 2. Results of measurements of cavitation induced turbulence in the wake of two ferries with either propeller or water jet truster.

	Propeller	**Water jet**
Geometry	Cylindrical	Conic
Width	8 m	6 m
Depth (max)	8−12 m	5−10 m
Core density	0−4 m	0−3 m (to 6 m)
Intensity (mode)	50 dB	48 dB
Duration	90 s	90 s

From the DBS data, filtered echograms are produced and shown in Figure 19. They show the echo intensity of the turbulent wake. The vortex produced by the propeller is clearly seen in Figure 19a). It is also found that the water jet wake spreads deeper down.

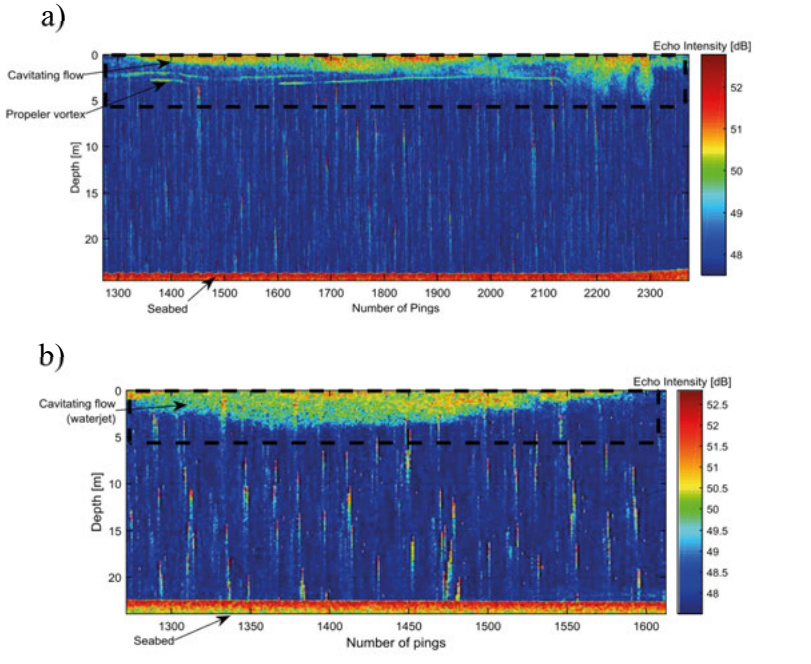

Figure 19. Filtered echograms from DBS data showing cavitating flow in the wake of a ferry with a) propeller and b) water jet thruster (Fig. 7 in Paper V).

5.4 Variability

5.4.1 Intermittent renewable energy

Variability has been studied for wind, solar, wave and tidal power. The difference in temporal variability between the four intermittent renewable sources is demonstrated in Figure 20 as reported in Paper VI. The energy content is normalized by the maximum available energy from each source and site respectively. The pattern clearly deviates between the sources. Solar energy has distinct time intervals for when its day or night and in the Nordic countries, also a large seasonal variation. Wind power fluctuates more randomly with a higher energy content during winter. A similar seasonal variation is seen for wave power but with more long-term fluctuations. The periodic pattern of tidal power is clearly visible in the right column.

These conditions will be important for a future aggregated power system and their consequences were further studied in Paper VII for the Nordic countries.

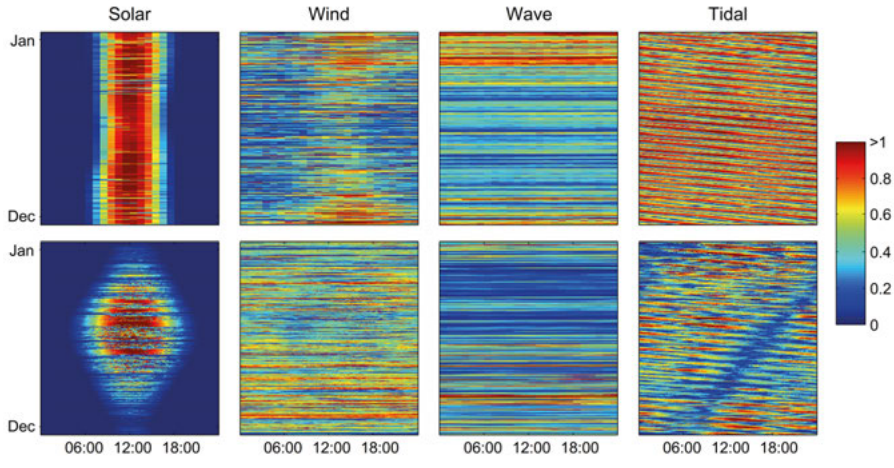

Figure 20. Variability of the natural resource for solar, wind, wave and tidal respectively. The top panel and bottom panel are examples from different sites around the globe, specified in Paper VI. (Fig. 2 in Paper VI).

From the study in Paper VII it was found that the four IRE sources have distinctly different variability patterns and different dominating frequency bands, as seen in Figure 21. For solar power (from photovoltaic systems, i.e. solar cells), 80% of the total standard deviation (σ_{raw} according to Eq. 4) comes from the short-term component. For wind power, the largest standard deviation is in the mid/short-term component while for wave and tidal it is for the long- and mid-term components respectively.

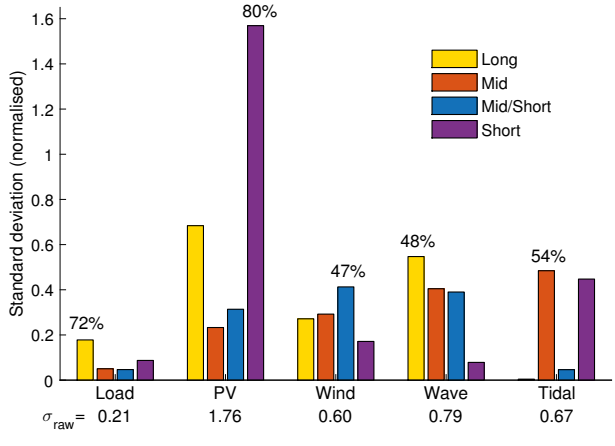

Figure 21. Standard deviation in power generation (σ, normalized to mean power generation) on different time scales for the four sources solar, wind, wave and tidal respectively (Fig. 2 in Paper VII).

In Fig. 3 in Paper VII the four sources are combined, as described in Section 4.3.1. When optimized for the long- or short-term component, wave power

has the highest share, whereas solar has the largest share for the mid- and mid/short-term components. Tidal energy has such a small total resource (3 TWh/year) that it only accounts for a small fraction of each mix.

It is seen in Figure 22 that the intermediate time scales may be more challenging, since it is on timescales between two days and four months that the largest increase in variability is seen for a high degree of IRE in the energy system. Short- and long-term variability, on the other hand, might not increase at all compared to today.

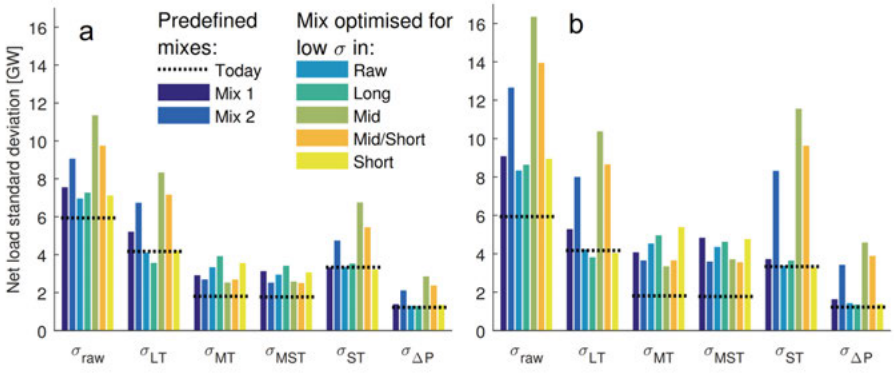

Figure 22. Net load standard deviations for the scenarios and mixes compared to today (Fig. 4 in Paper VII).

5.4.2 Aggregated tidal energy in Norway

For the tidal energy in Norway, the variability was first quantified for the natural case. The aggregated energy data was filtered at four different intervals to catch the daily variation and the spring/neap cycles. Figure 23 shows the variability for the total available energy, when aggregating all of the sites in the study separated for the four frequency bands according to:

The short-term component, less than 2 days (blue)
The mid/short-term component, for 2 days to 2 weeks (orange)
The mid-term component, for 2 weeks to 4 months (yellow)
The long-term component (purple)

The daily variation due to the semidiurnal tide is clearly seen in the short-term component. The monthly variations of the spring and neap tides can be discerned in the mid/short-term component and are clearly dominant in the mid-term component. The variation is negligible on longer time scales during one year.

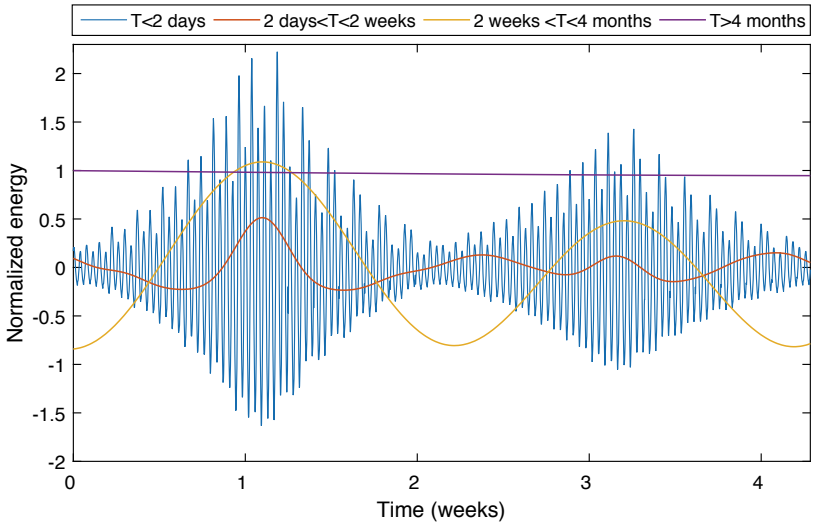

Figure 23. Normalized total available energy for the short-, mid/short-, mid-, and long-term components (Fig.4 Paper VIII).

It was found that a few of the sites contain a majority of the energy (Figure 11). They have the highest current speeds and the largest cross-sectional area. Their power outputs were limited in the Scenarios and the time lags were utilized to lower the variability as described in Section 4.3.2.

The standard deviations in energy are shown in Figure 24 a). The left column is the standard deviation in the natural resource. They are compared to the three scenarios. The largest deviations are seen in the short-term component and the mid-term component, as expected. The total standard deviation is the sum of its components squared (cf. Eq. 4). Scenario 2 has a significantly lower deviation in the short time component with a total standard deviation of $\sigma_{tot,2} = 0.738$.

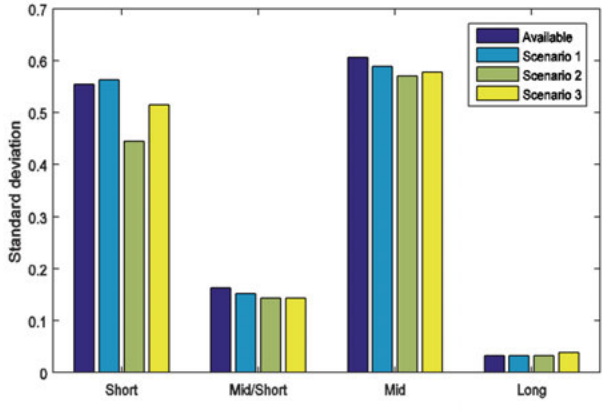

Figure 24. Standard deviation in energy for each of the four frequency bands and the three Scenarios (Fig. 5 in Paper VIII).

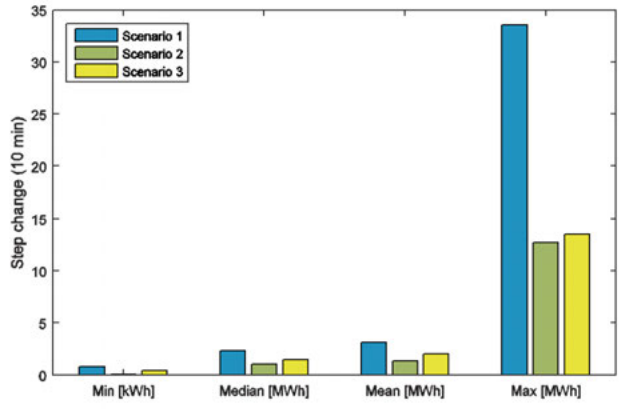

Figure 25. Minimum, median, mean and maximum values of the 10 minute step change (change in energy in 10 min steps) for the three Scenarios. (Fig. 6 in Paper VIII)

For Scenario 1, there were no smoothing on short time scales. The largest sites dominate the produced energy. A better result is obtained for Scenario 2, where the energy extraction is lower for the most energetic sites to better match the smaller sites. And indeed, the variability is lower for Scenario 2. In Scenario 3, the standard deviation is smaller than in the natural resource for all but the long-term component. However, a better smoothing would be obtained if the phasing would have been more favorable for the added sites.

The change in energy in 10 min steps is calculated for the three Scenarios. Figure 25 shows the statistical measures of the 10 minute step changes: the minimum value, the most common value, the mean and the maximum. The step changes are considerably smaller in the scenarios than in the natural resource with values of 2 kWh and 16, 21 and 231 MWh respectively.

The results show that Scenario 2 produces the least amount of energy (1.259 TWh/year). On the other hand, it has the least variability in terms of standard deviation and smallest step changes with a median value of 1.00 MWh (as compared to a mean produced energy of 24 MWh).

6. Conclusions

6.1 Tidal site: Characteristics and resource

There are many indications that the potential for marine current energy from tides is large in various areas around the world. Especially when the development of tidal turbines progresses towards turbines operating in more diverse flow conditions and depths. The measurement surveys performed at the tidal site Korsnesstraumen show that the site provides truly bi-directional flows with mean currents up to 2.06 m/s. Thus the site has potential for in-stream energy conversion. Similar conditions, a fjord inlet connecting the ocean to a basin, are expected at numerous sites along the Norwegian coast. It is thus probable that the potential for marine current energy is large in Norway.

The method of measuring along transects at a tidal site is a time and cost efficient way to perform an initial characterization of the natural flow. At sheltered sites, it is both convenient and sufficient to use a simple small sized boat to navigate across the site and to tow an ADCP. The instruments, i.e. the ADCPs, have performed well during the different measurement surveys. However, the importance of planning any measurement survey in detail and perform careful calibrations of the instrument are emphasized.

6.1.1 Simple prediction model

A simple prediction model was set up with the aim to predict peak current speed from tidal range. The assumption that the predicted tidal range in the charts coincides with the tidal range at the sill and that the tidal range controls the peak velocities at the site is shown to hold true. The proposed simple prediction model shows a strong linear relationship between tidal range and peak speed and allows prediction of peak speeds in the channel center within ±0.12 m/s These results, although site specific, show that the model can be used to predict the magnitude of peak current speed from information on tidal range at this and similar sites, i.e. tidal straits connecting the ocean to a bay or fjord.

Measurements of current velocity are, however, always required when performing a detailed characterization of a tidal site. A shortened measurement period is then economically beneficial. The model is shown to accurately (within 3% deviation) predict peak speeds in the channel center after 9 days of measurements. When implementing this model at another similar site, it is

thus suggested to perform measurements for at least 1/3 of the lunar tidal cycle around the time for the largest spring tide to make sure to catch both smallest and largest tidal ranges and thus smallest and largest peak speeds.

6.2 River site: Wake effects

The river site in Dalälven, Söderfors, is very advantageous as a test site due to the vicinity to the upstream hydro power plant. The power plant regulates the flow rate which results in steady and controllable flow speeds in the channel downstream. The successful deployment of the in-stream energy converter allows for important research on a prototype test station in its natural environment.

The performed measurement survey provides first results showing that the wake can be measured with the proposed technique, i.e. transect measurements following leading lines with positions recorded by a high accuracy positioning system. The wake can be seen to propagate approximately 6 to 7 turbine diameters downstream. However, more detailed studies are required to fully characterize the wake.

6.3 Ocean current site: Cavitation-induced flow

From the two measurement surveys the site was considered not to have potential for energy conversion due to its low current velocities.

The investigation of the cavitation-induced turbulence concluded that the MBS and DBS systems could detect and show the characteristics of the wake from the two different thruster mechanisms subject to the study. The wakes were found to reach depths of 10 m from propeller thrusters and 12 m from water jet thrusters and lasted for approximately 90 s. Thus, depending on the depth of the site, the turbulent wake may have an impact on marine current turbines placed in an area where ferries of the same type are present.

6.4 Variability

It can be concluded from the variability studies in Papers VI and VII that a wise combination of intermittent renewable energy (IRE) sources can lower the variability in net power generation on short and long time scales. An increase in net load variability on timescales between two days and four months is inevitable with a large amount of IRE. Thus, a fossil- and nuclear-free Nordic power system will increase the fluctuations with periods ranging from a few days to a few months, and increase the need for peak generating capacity. However, short- and long-term variability might not increase at all.

In Paper VIII it is shown that a majority of the tidal energy in Norway comes from a few of the most energetic sites. That is, sites with high current speeds and a large cross-sectional area. Variability in the power output can be lowered by aggregating a number of tidal energy sites with varying time lag. However, it is then crucial to choose sites with complementing time lag.

As expected, the daily variation is most profound, but also the spring/neap cycle will add a high degree of variability. It is the daily intermittency that can be smoothened by aggregating tidal sites of different phase. The key is to limit the power output from sites with high currents and thus high energy content. The large scale variability from spring and neap tides affect the whole region and can thus not be smoothened out.

The tidal phase shift in the studied area is substantial and well spread between the most energetic sites. Out of the investigated scenarios, Scenario 2 has the smallest variability, the smallest standard deviation and considerably smaller step changes.

7. Future studies

Resource characterizations at tidal current sites are still important for the understanding of tidal flows. Thus, a large scale measurement campaign quantifying the number of sites with potential for in-stream tidal current converters along the Norwegian coast would be interesting to perform. Required measurement methods are site specific, but the development of standardized techniques could still be beneficial.

The next step in the Söderfors project is to continue performing extended wake measurements as well as measurements of turbulence at and around the turbine and in the wake. Available data from logged velocity measurements upstream and downstream of the turbine in Söderfors can be used to investigate the natural flow affecting the turbine, e.g. distribution of current speeds. Lately, the focus is shifting towards characterizing the wakes of turbines in arrays or farms to improve the understanding of how turbines interact with the flow and the environment.

In the field of remote sensing of underwater phenomenon, it is obvious that Sonar measurements can provide detailed subsurface views and pictures. To further improve the results of the analysis of cavitation induced flow behind boats, the instruments may be deployed at the seabed to monitor the transiting of boats in greater detail. Sonar systems may also be used to investigate turbine wakes in greater details.

The study of tidal phasing in Norway may be improved by including analysis of local tidal constituents from each site when modelling the tide. A detailed study of the relationship between tide, tidal height and current velocities is also necessary. Furthermore, better optimization of the Scenarios could improve the results.

More research is needed that takes all intermittent renewable energy sources into account, with methods that use the same time resolution and analysis techniques so that the variability of all of the sources can be compared. A time interval of one hour or less is needed for it to be relevant for the power system. Moreover, it is important to have an energy system perspective when investigating how the sources can be combined and how smoothing of power output can be achieved. For the Nordic countries, ramping compensating possibilities in the power system should be examined.

Forecasting methods and accuracy were not examined for tidal energy in Paper VI and could therefore be interesting to look in to, to complement that study.

8. Summary of papers

PAPER I

Measurements of tidal current velocities in the Folda Fjord, Norway, with the use of a vessel mounted ADCP.

A tidal energy site in the Folda Fjord in Norway was investigated as a first step in evaluating its potential as a renewable energy resource. Transect measurements of flow velocities were performed with a vessel mounted ADCP.

The author has done most of the work in this paper.

The paper is published in *Proceedings of the ASME 2014 33rd International Conference on Ocean, Offshore and Arctic Engineering, Volume 8A: Offshore Engineering,* and was presented orally by the author in San Francisco, California, USA, June 10 2014.

PAPER II

Tidal resource characterization in the Folda Fjord, Norway.

The tidal site of the Folda Fjord was additionally investigated by deploying an ADCP for 54 days, measuring the flow characteristics. The data was analyzed in terms of characterizing metrics, and also used to develop a simple prediction model coupling tidal height to peak velocities at the site.

The author has done most of the work in this paper.

The paper is published in *International Journal of Marine Energy,* November 2015.

PAPER III

The Söderfors project: Experimental hydrokinetic power station deployment and first results.

This paper explains the deployment process of a marine current energy converter in the river Dalälven, which is part of the Söderfors project at Uppsala University. Also three ADCPs were deployed to monitor the water currents upstream and downstream of the turbine, as well as horizontally across the rotor plane.

The author was participating in the reassembling of the turbine blades, preparation of ADCPs for deployment and during the deployment of the converter and the measurement instruments.

The paper is published in *Proceedings of the 10th European Wave and Tidal Energy Conference Series, EWTEC 2013.*

PAPER IV

Studying the wake of a marine current turbine using an acoustic Doppler current profiler.

The wake characteristics of the flow behind the marine current energy converter in Söderfors was studied in this paper. Measurements of the velocity field were planned and conducted and the results give a first indication of the extent of the wake.

The author has contributed with writing the section about equipment, was responsible for setting up the ADCP and was participating in the collection of data.

The paper is published in *Proceedings of the 11th European Wave and Tidal Energy Conference Series, EWTEC 2015.*

PAPER V

Observation of cavitating flow using multibeam and dual-beam sonar systems: A comparison of wake strength caused by propelled vs waterjet thrusted vessels. In a marine renewable energy perspective (Part-a).

For a marine current turbine located in a waterway it is important to investigate what effect the presence of transiting boats may have on the turbine blades. In this paper, cavitation-induced turbulence in the wake of two ferries with different thrust mechanism was studied. With the use of a Multi-beam sonar and a Dual-beam sonar the extension and duration of the wake caused by first, a water jet and second a propeller driving mechanism was studied.

The author has contributed with assistance during field work, proofreading and commenting on the paper.

The paper was resubmitted after revision to *Journal of Marine Science and Engineering*, April 2017.

Paper VI

Variability assessment and forecasting of renewables: A review for solar, wind, wave and tidal resources.

This review paper discusses the variability of the renewable resources of solar, wind, wave and tidal energy. The spatial and temporal variability was reviewed and compared between the different sources. The variability of the tidal resource is mainly due to four aspects; tidal regime, the tidal cycle, bathymetry at the site and weather effects. Consequences of including such variable sources into the existing power systems is discussed.

The author was responsible for the tidal resource parts.

The paper is published in *Renewable & Sustainable Energy Reviews*, April 2015.

Paper VII

Net load variability in Nordic countries with a highly or fully renewable power system.

The net load variability from wind, solar, wave and tidal energy is studied for the Nordic countries, to investigate what effect a larger share of intermittent renewable energy would have on the variability in the electricity grid. All four sources are modeled and the variability, in terms of standard deviation and step change, is studied for each of the sources and for all of the sources combined. The variability on different time scales is studied through frequency analysis and a few scenarios are presented, as well as mixes optimized for a small standard deviation.

The author was responsible for the tidal resource parts: collecting data, and setting up and describing the model.

The paper is published in *Nature Energy*. November 2016.

Paper VIII

Tidal Current Phasing Along the Coast of Norway.

This paper discusses how the effects of tidal current phasing along the coast of Norway can be used to get a more smooth power output if a large number of tidal energy plants would be aggregated. Data on tidal current peak speed was collected at 114 sites, velocity time series was modeled and the available energy calculated. In three scenarios, the variability of the aggregated energy was analyzed and compared to the variability of the natural resource.

The author has done most of the work in this paper.

The paper is published in *Proceedings of the 3^{d} Asian Wave and Tidal Energy Conference Series, AWTEC 2016.*

9. Svensk sammanfattning

Att producera elektricitet från förnybara energikällor är ett forskningsområde som utvecklas kontinuerligt. Inom det område som kallas marin strömkraft innebär det att omvandla den kinetiska energin i vattenströmmar till elektricitet. Vattenströmmarna är framförallt orsakade av tidvatten som beror på månens och solens dragningskraft, samt jordens rotation. När tidvattnet stiger (vid flod) pressas vattnet in i fjordar, runt uddar och genom sund vilket innebär att det bildas vattenströmmar. Detsamma sker när tidvattnet sjunker (vid ebb) men i motsatt riktning. Tidvattenvågen färdas över haven och når olika ställen av kusten vid olika tidpunkt. Högvatten inträffar med andra ord med en viss tidsförskjutning på olika platser. Energin i vattenströmmarna är proportionell mot hastigheten i kubik. Genom att placera vindkraftsliknande turbiner på platser med höga vattenhastigheter så kan man utvinna förnyelsebar energi. Dock kommer turbinen påverka flödet nedström, i dess vak, där turbulens bildas och vattenhastigheten sjunker tillfälligt.

Turbinerna som används inom området marin strömkraft står i startgroparna till att ta steget från prototyp till kommersiell produkt. Dock pågår fortfarande forskning för att till fullo förstå tidvattenresursens egenskaper och vilken påverkan en tidvattenturbin har på vattenflödet. Därför krävs noggranna undersökningar av flödet på varje plats som har potential för energiutvinning. Att tillhandahålla data av hög kvalitet från mätningar av vattenhastigheten är därför av stor betydelse.

Mätningarna har utförts med ett instrument som sänder ut ljudpulser av en viss frekvens. Dessa reflekteras på partiklar i vattnet och vattnets hastighet beräknas utifrån Dopplerskiftet i frekvensen. På så sätt fås en hastighetsprofil av vattenkolumnen (med andra ord hastigheten på olika djup). Instrumentet kan antingen placeras på botten för att ge långtidsmätningar eller monteras i en lite flytande katamaran och dras tvärs över eller längs med vattenflödet.

I denna avhandling har mätningar av flödeshastigheter utförts på tre typer av platser. En plats med tidvattenströmmar, belägen i en fjord i Norge, har undersökts för sin resurspotential. Mätningar av vattenhastigheten utfördes för att kartlägga resursens variation i både tid och rum. Resultaten visar vattenhastigheter i storleksordningen 2 m/s i mitten av kanalen. Dessutom uppvisar flödet liten variation från huvudriktningen för både inkommande (flod) och utgående (ebb) flöden, något som ofta är fördelaktigt för tidvattenturbiner. Platsen har således potential för energiomvandling av fritt strömmande vatten.

I en älv har ett marint strömkraftverk placerats och platsen har fungerat som experimentområde. Strömkraftverket, som har en vertikalaxlad turbin, har utvecklats vid Uppsala universitet och sjösatts i Dalälven, Söderfors inom ett projekt som går under namnet *Söderforsprojektet*. Vattenflödet på platsen regleras uppströms av ett närliggande vattenkraftverk. Turbinen har körts i jämnt flöde och mätningar har utförts för att karaktärisera vakens utbredning samt att utvärdera mätmetoden.

På en plats med havsströmmar undersöktes bland annat vilken påverkan passerande färjor kan ha på objekt, t.ex. turbiner, placerade under vattnet. Mätningar genomfördes med två olika typer av ekolod för att få fram en undervattensbild av vaken från en propellerdriven respektive en vattenjet-driven färja. Båda typerna av vakar var tydligt synliga och sågs sträcka sig från ytan ner till ca 10 m djup.

Utöver fältarbetet beskrivet ovan så har även variabiliteten av de oregelbundna förnybara energikällorna vind-, sol-, våg- och tidvattenenergi i de Nordiska länderna undersöktes. Variabiliteten för var och en av resurserna har distinkt olika egenskaper, vilket är fördelaktigt när man kombinerar effekten producerad från dem. Tidvattenvariabiliteten beror huvudsakligen på fyra egenskaper: antalet hög- och lågvatten per dag, tidvattencykeln över en månad, djupförhållandena på platsen som ger turbulens och vädereffekter.

I undersökningen modellerades effektproduktionen från de fyra förnyelsebara resurserna var och en för sig för att sedan kombineras på olika sätt i ett ”mycket förnybart” och ett ”helt förnybart” scenario. Genom att analysera den totala uteffekten i olika tidskomponenter (långsamma, medellånga, medel/korta och korta tidskomponenter) så var det möjligt att minimera variabiliteten på olika tidsskalor.

Tidvattenvariabiliteten i Norge undersöktes sedan separat. Det faktum att tidvattenströmmar är förutsägbara har stora fördelar vid planering av elektricitetstillgången från tidvattenturbiner. Dock varierar tidvattenströmmarna kontinuerligt mellan maximal strömhastighet till nästan stillastående vid hög- och lågvatten. Det skulle innebära att en större mängd reservkraft eller energilagring krävs för att kompensera för variationen i uteffekten från maximal till minimal produktion som sker flera gånger per dag. Tidsförskjutningen mellan platser längs den norska kusten ger en utjämnande effekt på tidsperioder om några timmar men eftersom tidvattencykeln, med springflod och nipflod var fjortonde dag, påverkar ett större område samtidigt så kan inte den storskaliga tillgången på tidvattenkraft utjämnas.

10. Acknowledgement

I would like to thank my supervisors Karin Thomas, Sandra Eriksson and Mats Leijon for your supervision and for giving me the opportunity to work within these projects and perform all the field work, it has been a great learning experience. The following are acknowledged for their financial support: The Carl Trygger Foundation for Scientific Research, the Swedish Energy Agency (Swedish Centre for Renewable Electric Energy Conversion, CFE III), StandUp for Energy, the Swedish Research Council, the ÅForsk Foundation, the J. Gust. Richert Memorial Fund, the C. F. Liljewalchs stipendiestiftelse and the Bixia Environmental Fund.

Big thanks to present and former members of the marine current-group, Johan Forslund, Anders Goude, Minh Thao Nguyen, Emilia Lalander, Staffan Lundin, Mårten Grabbe and Katarina Yuen, for all the hard work in making the Söderfors-project a reality. Without you I would never have had the chance to mount turbine blades at the parking lot of ICA in Söderfors, watch a marine current energy converted being lift off a bridge, chug about in a boat at Dalälven in November, or drive 900 km to a fjord in Norway to deploy an ADCP. Also thanks to Francisco Francisco and Irina Dolguntseva for your collaboration. Thanks to those who assisted during planning and execution of measurements in Foldafjorden, Dalälven and/or Finnhamn (the Stockholm archipelago was beautiful in winter too). Thanks to Rafael and Kaspars; my roommates: Valeria, Liselotte, Stefan, Linnéa and Fredrik; and to the rest of my friends and colleagues for creating such a friendly atmosphere at the Division of Electricity. It has been a memorable time, working alongside all of you talented people.

Also thanks to Sofia Kontos, Tobias Kamf and Jennifer Leijon for your friendship, moral support and numerous walks in the sun – I could never have done this without you guys. A special thanks to Martin Adolphson for your love and support. You have been there for me every step of the way, even as chauffeur and my helping hand during the recovery of the ADCP in Norway (indeed, the Norwegian Sea is cold even in August!). Lastly, thanks to my family and to Sandra Aljija for always supporting me through good times and through bad.

I made it!

11. References

[1] World Energy Council *Renewables integration. Variable renewables integration in electricity systems: How to get it right*. 62-64 Cornhill, London EC3V 3NH, United Kingdom: World Energy Council; 2016.

[2] World Energy Council *World Energy Resources - Marine Energy*. 62-64 Cornhill, London EC3V 3NH, United Kingdom: World Energy Council; 2016.

[3] Kempener R., Neumann F. *Tidal Energy - Technology Brief*. International Renewable Energy Agency (IRENA); 2014.

[4] REN21 (Renewable Energy Policy Network for the 21st Century) *Renewables 2016 Global Status Report*. 2016.

[5] Garrett C., Cummins P. The power potential of tidal currents in channels. *Proc R Soc A* 2005; (461): 2563–72. Doi: 10.1098/rspa.2005.1494.

[6] Garrett C., Cummins P. Limits to tidal current power. *Renew Energy* 2008; 33(11): 2485–90. Doi: 10.1016/j.renene.2008.02.009.

[7] Garrett C., Cummins P. Maximum power from a turbine farm in shallow water. *J Fluid Mech* 2013; 714: 634–43. Doi: 10.1017/jfm.2012.515.

[8] Vennell R. Tuning turbines in a tidal channel. *J Fluid Mech* 2010; 663: 253–67. Doi: 10.1017/S0022112010003502.

[9] Vennell R. Estimating the power potential of tidal currents and the impact of power extraction on flow speeds. *Renew Energy* 2011; 36(12): 3558–65. Doi: 10.1016/j.renene.2011.05.011.

[10] Vennell R. Tuning tidal turbines in-concert to maximise farm efficiency. *J Fluid Mech* 2011; 671: 587–604. Doi: https://doi.org/10.1017/S0022112010006191.

[11] Vennell R. Realizing the potential of tidal currents and the efficiency of turbine farms in a channel. *Renew Energy* 2012; 47: 95–102. Doi: 10.1016/j.renene.2012.03.036.

[12] Vennell R. The energetics of large tidal turbine arrays. *Renew Energy* 2012; 48: 210–9. Doi: 10.1016/j.renene.2012.04.018.

[13] Vennell R. Exceeding the Betz limit with tidal turbines. *Renew Energy* 2013; 55: 277–85. Doi: 10.1016/j.renene.2012.12.016.

[14] Vennell R., Funke SW., Draper S., Stevens C., Divett T. Designing large arrays of tidal turbines: A synthesis and review. *Renew Sustain Energy Rev* 2015; 41: 454–72. Doi: 10.1016/j.rser.2014.08.022.

[15] Lewis M., Neill SP., Robins PE., Hashemi MR. Resource assessment for future generations of tidal-stream energy arrays. *Energy* 2015; 83: 403–15. Doi: 10.1016/j.energy.2015.02.038.

[16] Frost C., Morris CE., Mason-Jones A., O'Doherty DM., O'Doherty T. The effect of tidal flow directionality on tidal turbine performance characteristics. *Renew Energy* 2015; 78: 609–20. Doi: 10.1016/j.renene.2015.01.053.

[17] Evans P., Mason-Jones A., Wilson C., Wooldridge C., O'Doherty T., O'Doherty D. Constraints on extractable power from energetic tidal straits. *Renew Energy* 2015; 81: 707–22. Doi: 10.1016/j.renene.2015.03.085.

[18] Gunawan B., Neary VS., Colby J. Tidal energy site resource assessment in the East River tidal strait, near Roosevelt Island, New York, New York. *Renew Energy* 2014; 71: 509–17. Doi: 10.1016/j.renene.2014.06.002.
[19] O'Rourke F., Boyle F., Reynolds A. Ireland's tidal energy resource; An assessment of a site in the Bulls Mouth and the Shannon Estuary using measured data. *Energy Convers Manag* 2014; 87: 726–34. Doi: 10.1016/j.enconman.2014.06.089.
[20] Palodichuk M., Polagye B., Thomson J. Resource mapping at tidal energy sites. *IEEE J Ocean Eng* 2013; 38(3): 433–46. Doi: 10.1109/JOE.2012.2227578.
[21] Goddijn-Murphy L., Woolf DK., Easton MC. Current patterns in the Inner Sound (Pentland Firth) from underway ADCP data. *J Atmospheric Ocean Technol* 2013; 30(1): 96–111. Doi: 10.1175/JTECH-D-11-00223.1.
[22] Fairley I., Evans P., Wooldridge C., Willis M., Masters I. Evaluation of tidal stream resource in a potential array area via direct measurements. *Renew Energy* 2013; 57: 70–8. Doi: 10.1016/j.renene.2013.01.024.
[23] Polagye B., Thomson J. Tidal energy resource characterization: Methodology and field study in Admiralty Inlet, Puget Sound, WA (USA). *J Power and Energy* 2013; 227(3): 252–367. Doi: 10.1177/0957650912470081.
[24] Work PA., Haas KA., Defne Z., Gay T. Tidal stream energy site assessment via three-dimensional model and measurements. *Appl Energy* 2013; 102: 510–9. Doi: 10.1016/j.apenergy.2012.08.040.
[25] Lee J., Webb BM., Dzwonkowski B., Park K., Valle-Levinson A. Bathymetric influences on tidal currents at the entrance to a highly stratified, shallow estuary. *Cont Shelf Res* 2013; 58: 1–11. Doi: 10.1016/j.csr.2013.03.002.
[26] Epler J., Polagye B., Thomson J. Shipboard acoustic Doppler current profiler surveys to assess tidal current resources. *OCEANS 2010*. 2010. p. 1–10.
[27] Neary VS., Gunawan B., Richmond MC., Durgesh V., Polagye B., Thomson, Jim., Muste M., Fontaine A. *Field measurements at river and tidal current sites for hydrokinetic energy development: Best practices manual*. Oak Ridge National Laboratory, UT-Battelle; 2011.
[28] Bryden IG., Couch SJ., Owen A., Melville G. Tidal current resource assessment. *Proc Inst Mech Eng Part J Power Energy* 2007; 221(2): 125–35. Doi: 10.1243/09576509JPE238.
[29] Fröberg E. *Current power resource assessment - A study of selected sites in Sweden and Norway*. MSc, Uppsala University and Swedish University of Agricultural Sciences, Uppsala, Sweden, 2006.
[30] Muste M., Yu K., Spasojevic M. Practical aspects of ADCP data use for quantification of mean river flow characteristics; Part I: Moving-vessel measurements. *Flow Meas Instrum* 2004; 15(1): 1–16. Doi: 10.1016/j.flowmeasinst.2003.09.001.
[31] Vennell R. Acoustic Doppler Current Profiler measurements of tidal phase and amplitude in Cook Strait, New Zealand. *Cont Shelf Res* 1994; 14(4): 353–64. Doi: 10.1016/0278-4343(94)90023-X.
[32] Lewis MJ., Neill SP., Hashemi MR., Reza M. Realistic wave conditions and their influence on quantifying the tidal stream energy resource. *Appl Energy* 2014; 136: 495–508. Doi: 10.1016/j.apenergy.2014.09.061.
[33] Frost C., Evans P., Mason-Jones A., O'Doherty T., O'Doherty D. The effect of axial flow misalignment on tidal turbine performance. *1st International Conference on Renewable Energies Offshore*. Lisbon, Portugal; 2014.
[34] Iyer AS., Couch SJ., Harrison GP., Wallace AR. Variability and phasing of tidal current energy around the United Kingdom. *Renew Energy* 2013; 51: 343–57. Doi: 10.1016/j.renene.2012.09.017.

[35] Harding SF., Bryden IG. Directionality in prospective Northern UK tidal current energy deployment sites. *Renew Energy* 2012; 44: 474–7. Doi: 10.1016/j.renene.2012.02.003.
[36] Neill SP., Hashemi MR., Lewis MJ. The role of tidal asymmetry in characterizing the tidal energy resource of Orkney. *Renew Energy* 2014; 68: 337–50. Doi: 10.1016/j.renene.2014.01.052.
[37] Hashemi MR., Neill SP., Robins PE., Davies AG., Lewis MJ. Effect of waves on the tidal energy resource at a planned tidal stream array. *Renew Energy* 2015; 75: 626–39. Doi: 10.1016/j.renene.2014.10.029.
[38] Lynge BK., Hjelmervik K., Gjevik B. Storm surge and tidal interaction in the Tjeldsund channel, northern Norway. *Ocean Dyn* 2013; 63(7): 723–39. Doi: 10.1007/s10236-013-0625-1.
[39] Gjevik B., Flather RA., Hareide D. Sea-level oscillations with 6-h period in the North Sea 29-31 October 2000. An analysis of data from stations in the northern North Sea and along the western coast of Norway. *Ocean Dyn* 2004; 54: 477–88. Doi: 10.1007/s10236-004-0093-8.
[40] Gjevik B., Hareide D. Ekstrem vannstandsendring og strom i Oslofjorden natten mellom 3. og 4. desember 1999. *Naturen Univ* 2000; 5: 258–63.
[41] Bryden IG., Grinsted T., Melville G. Assessing the potential of a simple channel to deliver useful energy. *Appl Ocean Res* 2004; 26(5): 198–204. Doi: http://dx.doi.org/10.1016/j.apor.2005.04.001.
[42] Blunden LS., Bahaj AS. Effects of tidal energy extraction at Portland Bill, southern UK predicted from a numerical model. *Proceedings of the 7th European Wave and Tidal Energy Conference*. Porto, Portugal; 2007.
[43] Adcock TAA., Draper S. Power extraction from tidal channels – Multiple tidal constituents, compound tides and overtides. *Renew Energy* 2014; 63: 797–806. Doi: 10.1016/j.renene.2013.10.037.
[44] Lalander E., Leijon M. Numerical modeling of a river site for in-stream energy converters. *Proceedings of the 8th European Wave and Tidal Energy Conference*. Uppsala, Sweden; 2009.
[45] Lalander E., Leijon M. In-stream energy converters in a river - Effects on upstream hydropower station. *Renew Energy* 2011; 36(1): 399–404. Doi: http://dx.doi.org/10.1016/j.renene.2010.05.019.
[46] Yuen K., Lundin S., Grabbe M., Lalander E., Goude A., Leijon M. The Söderfors Project: Construction of an experimental hydrokinetic power station. *Proceedings of the 9th European Wave and Tidal Energy Conference*. Southampton, UK; 2011.
[47] Grabbe M., Yuen K., Goude A., Lalander E., Leijon M. Design of an experimental setup for hydro-kinetic energy conversion. *Int J Hydropower Dams* 2009; 16(5): 112–6.
[48] Lundin S., Forslund J., Goude A., Grabbe M., Yuen K., Leijon M. Experimental demonstration of performance of a vertical axis marine current turbine in a river. *J Renew Sustain Energy* 2016; 8(6). Doi: http://dx.doi.org/10.1063/1.4971817.
[49] Lundin S., Goude A., Leijon M. One-dimensional modelling of marine current turbine runaway behaviour. *Energies* 2016; 9(309). Doi: doi:10.3390/en9050309.
[50] Forslund J., Lundin S., Thomas K., Leijon M. Experimental results of a DC bus voltage level control for a load-controlled marine current energy converter. *Energies* 2015; 8: 4572–86. Doi: doi:10.3390/en8054572.
[51] Apelfröjd S., Ekström R., Thomas K., Leijon M. A Back-to-Back 2L-3L Grid Integration of a Marine Current Energy Converter. *Energies* 2015; 8(2): 808–20. Doi: 10.3390/en8020808.

[52] Lundin S. *Marine Current Energy Conversion*. PhD dissertation, Uppsala University, Uppsala, Sweden, 2016.
[53] Lalander E. *Hydrokinetic Resource Assessment : Measurements and Models*. PhD dissertation, Uppsala University, Uppsala, Sweden, 2013.
[54] Grabbe M. *Hydro-Kinetic Energy Conversion : Resource and Technology*. PhD dissertation, Uppsala University, Uppsala, Sweden, 2013.
[55] Yuen K. *System Perspectives on Hydro-Kinetic Energy Conversion*. PhD dissertation, Uppsala University, Uppsala, Sweden, 2012.
[56] Goude A. *Fluid Mechanics of Vertical Axis Turbines : Simulations and Model Development*. PhD dissertation, Uppsala University, Uppsala, Sweden, 2012.
[57] Thomas K. *Low Speed Energy Conversion from Marine Currents*. PhD dissertation, Uppsala University, Uppsala, Sweden, 2007.
[58] Segergren E. *Direct Drive Generator for Renewable Power Conversion from Water Currents*. PhD dissertation, Uppsala University, Uppsala, Sweden, 2005.
[59] Grabbe M., Lalander E., Lundin S., Leijon M. A review of the tidal current energy resource in Norway. *Renew Sustain Energy Rev* 2009; 13(8): 1898–909. Doi: 10.1016/j.rser.2009.01.026.
[60] Pugh D. *Changing sea levels: Effects of tides, weather and climate*. Cambridge, U.K.: Cambridge University Press; 2004.
[61] Hicks SD. *Understanding tides*. U.S. Dept. of Commerce, National Oceanic and Atmospheric Administration (NOAA), National Ocean Service, Center for Operational Oceanographic Products and Services; 2006.
[62] Polagye BL., Epler J., Thomson J. Limits to the predictability of tidal current energy. *OCEANS 2010*. 2010. p. 1–9.
[63] Bahaj AS., Myers LE., Thomson MD., Jorge N. Characterising the wake of horizontal axis marine current turbines. *7th European Wave and Tidal Energy Conference*, vol. 2007. Porto, Portugal; 2007.
[64] Turnock SR., Phillips AB., Banks J., Nicholls-Lee R. Modelling tidal current turbine wakes using a coupled RANS-BEMT approach as a tool for analysing power capture of arrays of turbines. *Ocean Eng* 2011; 38(11–12): 1300–7. Doi: 10.1016/j.oceaneng.2011.05.018.
[65] Tedds SC., Owen I., Poole RJ. Near-wake characteristics of a model horizontal axis tidal stream turbine. *Renew Energy* 2014; 63: 222–35. Doi: 10.1016/j.renene.2013.09.011.
[66] Bachant P., Wosnik M. Characterising the near-wake of a cross-flow turbine. *J Turbul* 2015; 16(4): 392–410. Doi: http://dx.doi.org/10.1080/14685248.2014.1001852.
[67] Brennan C., Colonius T., Wang YC., Preston A. Cloud cavitation phenomena. The National Academy of Science; 2000.
[68] Lauterborn W., Ohl C-D. Cavitation bubble dynamics. *Ultrason Sonochemistry* 1997; 4: 65–75. Doi: 1350-4177/97/.
[69] Soloviev A., Maingot C., Agor M., Nash L., Dixon K. 3D Sonar measurements in wakes of ships of opportunity. *J Atmospheric Ocean Technol* 2012; 29(6): 880–6. Doi: 10.1175/JTECH-D-11-00120.1.
[70] Sinden G. *Variability of UK Marine Resources*. Environmental Change Institute & The Carbon Trust; 2005.
[71] Giorgi S., Ringwood JV. Can tidal current energy provide base load? *Energies* 2013; 6: 2840–58. Doi: doi:10.3390/en6062840.
[72] Coker P., Barlow J., Cockerill T., Shipworth D. Measuring significant variability characteristics: An assessment of three UK renewables. *Renew Energy* 2013; 53: 111–20. Doi: 10.1016/j.renene.2012.11.013.

[73] Jacobson MZ., Delucchi MA., Bazouin G., Bauer ZAF., Heavey CC., Fischer E., Morris SB., Piekutowski DJY., Vencill TA., Yeskoo TW. 100% clean and renewable wind, water, and sunlight (WWS) all-sector energy roadmaps for the 50 United States. *Energy Environ Sci* 2015; 8: 2093–117. Doi: 10.1039/c5ee01283j.
[74] Polagye B., Thomson J. Implications of tidal phasing for power generation at a tidal energy site. *Proceedings of the 1sr Marine Energy Technology Symposium (METS13)*. Washington, D.C.; 2013.
[75] Clarke JA., Connor G., Grant AD., Johnstone CM. Regulating the output characteristics of tidal current power stations to facilitate better base load matching over the lunar cycle. *Renew Energy* 2006; 31: 173–80. Doi: 10.1016/j.renene.2005.08.024.
[76] Hardisty J. Power intermittency, redundancy and tidal phasing around the United Kingdom. *Geogr J* 2008; 174(1): 76–84. Doi: http://www.jstor.org/stable/30139406.
[77] Neill SP., Hashemi MR., Lewis MJ. Optimal phasing of the European tidal stream resource using the greedy algorithm with penalty function. *Energy* 2014; 73: 997–1006. Doi: 10.1016/j.energy.2014.07.002.
[78] Neill SP., Hashemi MR., Lewis MJ. Tidal energy leasing and tidal phasing. *Renew Energy* 2016; 85: 580–7. Doi: http://dx.doi.org/10.1016/j.renene.2015.07.016.
[79] Black & Veatch Ltd., Carbon Trust *Tidal stream - Phase I - Tidal stream energy resource and technology summary report*. 2004.
[80] Black & Veatch Ltd., Carbon Trust *Tidal stream - Phase II - UK tidal stream energy resource assessment*. Isleworth, United Kingdom; 2005.
[81] Bryden IG., Couch SJ. How much energy can be extracted from moving water with a free surface: A question of importance in the field of tidal current energy? *Renew Energy* 2007; 32: 1961–6. Doi: 10.1016/j.renene.2006.11.006.
[82] Legrand C. *Assessment of tidal energy resource - Marine renewable energy guides*. London: The European Marine Energy Centre Ltd (EMEC); 2009.
[83] Francisco F., Sundberg J. Sonar for environmental monitoring. Initial setup of an active acoustic platform. *25th International Ocean and Polar Engineering Conference Kona, Big Island, Hawaii, USA, June 21-26, 2015*. International Society of Offshore and Polar Engineers (ISOPE); 2015.
[84] Francisco F., Sundberg J. Sonar for Environmental Monitoring: Construction of a multifunctional active acoustic platform applied for marine renewables. *Preprints* 2016. Doi: 10.20944/preprints201611.0064.v1.
[85] *Den Norske Los 4 - Farvannsbeskrivelse Stad-Rorvik*. vol. 4. 6th ed. Stavanger: Statens kartverk Sjokartverket; 2003.
[86] Teledyne RD Instruments, Inc. WorkHorse Monitor/Sentinel User's Guide 2007.
[87] Teledyne RD Instruments, Inc. Acoustic Doppler Current Profiler, Principles of Operation, A Practical Primer 2011.
[88] Gooch S., Thomson J., Polagye B., Meggitt D. Site characterization for tidal power. *OCEANS 2009, MTS/IEEE Biloxi - Marine Technology for Our Future: Global and Local Challenges*. 2009. p. 1–10.
[89] Thomson RE., Emery WJ. *Data analysis methods in physical oceanography*. vol. 2014. 3rd ed. Amsterdam, The Netherlands: Elsevier; n.d.
[90] Pawlowicz R., Beardsley B., Lentz S. Classical tidal harmonic analysis including error estimates in MATLAB using T_TIDE. *Comput Geosci* 2002; 28(8): 929–37. Doi: 10.1016/S0098-3004(02)00013-4.

[91] The Norwegian Mapping Authority Water level and tidal information. *Se Havnivå*. http://kartverket.no/sehavniva. [accessed June 18, 2015].
[92] Carpman N. *Potentialbedömningar av marin strömkraft i Finnhamn - Fältmätningar och resultat*. Box 534, 752 21 Uppsala, Sweden: Uppsala University; 2015.
[93] *Den Norske Los 3 - Farvannsbeskrivelse Jaerens rev-Stad*. vol. 3. 6th ed. Stavanger: Statens kartverk Sjokartverket; 2006.
[94] *Den Norske Los 5 - Farvannsbeskrivelse Rorvik-Lodingen og Andenes*. vol. 5. 6th ed. Stavanger: Statens kartverk Sjokartverket; 2001.
[95] *Den Norske Los 6 - Farvannsbeskrivelse Lodingen og Andenes - Grense-Jakobselv*. vol. 6. 5th ed. Stavanger: Statens kartverk Sjokartverket; 1999.

Acta Universitatis Upsaliensis

Digital Comprehensive Summaries of Uppsala Dissertations from the Faculty of Science and Technology 1499

Editor: The Dean of the Faculty of Science and Technology

A doctoral dissertation from the Faculty of Science and Technology, Uppsala University, is usually a summary of a number of papers. A few copies of the complete dissertation are kept at major Swedish research libraries, while the summary alone is distributed internationally through the series Digital Comprehensive Summaries of Uppsala Dissertations from the Faculty of Science and Technology. (Prior to January, 2005, the series was published under the title "Comprehensive Summaries of Uppsala Dissertations from the Faculty of Science and Technology".)

Distribution: publications.uu.se
urn:nbn:se:uu:diva-319033

ACTA
UNIVERSITATIS
UPSALIENSIS
UPPSALA
2017